Investigations of nuclear structure with allowance for the continuum

I. Rotter

Central Institute of Nuclear Research, Rossendorf, Dresden, German Democratic Republic
Fiz. Elem. Chastits At. Yadra **15**, 762–807 (July–August 1984)

Studies of the influence of the continuous spectrum (the continuum) on the properties of discrete nuclear states in the framework of the nuclear shell model are reviewed. Coupling between the discrete states and the continuum leads to the appearance of an additional term in both the Hamiltonian and the discrete-state wave function. These terms characterize the finiteness of the nucleus. They are responsible for a definite breaking of the symmetry of the residual nuclear interaction, such as breaking of the charge symmetry, and they describe the nuclear surface. The energies and widths of the nuclear states are determined by complex eigenvalues of the nuclear Hamiltonian. It is shown that the partial widths factorize in the form of a product of a spectroscopic factor and a penetrability factor under the condition that the spectroscopic factor is large. An expression is obtained for the S matrix containing not only the so-called resonance parameters but also functions calculated in the framework of the model. The shape of the resonances is sensitive to these functions. In some cases, the resonances may appear in the form of cusps. These conclusions are confirmed by the results of numerical calculations.

INTRODUCTION

In attempting to describe a finite nuclear system, we encounter the problem of solving the Schrödinger equation $(H-E)\Psi=0$ using a basis of wave functions that contains states which depend on energies both discretely and continuously. Since the two types of wave functions have different mathematical properties, this problem can be solved algebraically only approximately. It is therefore not surprising that in nuclear physics two directions have arisen—investigation of nuclear structure restricted to the properties of the discrete states, and nuclear reactions, in which the properties of the continuum states are studied. The Schrödinger equation is solved correspondingly using sets of wave functions that depend on the energy discretely or continuously. The influence of states of the one kind on the other is taken into account approximately. Although this method of solution leads, as a rule, to good quantitative agreement with experiment, some basic problems have not yet been solved.

One such problem is the calculation of the lifetime of a nuclear state. The structure of the state is calculated using a Hamiltonian that is a Hermitian operator in the subspace of the wave functions of the discrete spectrum. The eigenvalues of this Hamiltonian are real and are interpreted as the energies of the excited nuclear states. The lifetime of the excited nuclear states can be estimated by means of overlap structure integrals (spectroscopic factors) and penetrability factors. It is not surprising that the results obtained in this manner describe the experimental data only partly. For example, the problem of α decay of heavy nuclei has not yet been solved despite the fact that it is one of the oldest problems in nuclear physics and the subject of much effort.

Since the majority of excited states of finite nuclei decay by the emission of one particle, the Hamiltonian describing the nuclear structure must be a non-Hermitian operator that goes over into a Hermitian operator when the bound states lie below the particle-emission threshold. Then the imaginary parts of the eigenvalues of the Hamiltonian describe the lifetimes of the corresponding nuclear states, while the real part determines their energies. The non-Hermitian part of the Hamiltonian cannot be completely reproduced solely by introducing an additional term into the two-particle residual forces, since it characterizes the many-particle nature of the finite nucleus. The non-Hermitian part of the Hamiltonian depends, for example, on the decay threshold energies. There is no analog of this in nuclear matter, and this is therefore a specific feature of finite nuclei.

The condition that the Hamiltonian for finite nuclei must be a non-Hermitian operator is not taken into account in any of the existing calculations of nuclear structure. The results of such calculations with a Hermitian Hamiltonian give discrete energies for all excited nuclear states. They are to be regarded as a first approximation to the solution of the problem. Allowance for the continuum leads to corrections that influence not only the decay states but also the bound states lying below the threshold for the emission of one particle. Finally, the lifetimes of the decay states can now be expressed in terms of the imaginary parts of the eigenvalues of the Hamiltonian.

The aim of the present paper is to review the influence of the continuum states on the structure of nuclear states. In Sec. 1 we consider a formalism (the shell model in the continuum) that makes it possible to take into account states with one particle in the continuum. Spectroscopic characteristics such as the energy, width, and wave function of a nuclear state are determined in Sec. 2. We then derive an expression for the S matrix in terms of functions that determine the energy and width of a state. Their significance is clarified by analyzing the line shape of an isolated resonance. In Sec. 3 we consider the symmetry breakings due to the finiteness of the nucleus. Such symmetry breaking does not occur in nuclear matter. We discuss surface effects in finite nuclei. The conclusions about the mutual influence of the discrete and continuum states are given in the last section.

 0090-4759/84/040341-20$04.40

1. THE SHELL MODEL IN THE CONTINUUM

Formulation of the Approach

The shell model in the continuum formulated by Barz *et al.*[1] is a formalism for solving the Schrödinger equation for both discrete and continuum states. It is based, on the one hand, on the shell-model approach to nuclear reactions developed by Mahaux and Weidenmüller[2] and, on the other, on the truncation technique for single-particle resonances proposed by Wang and Shakin.[3] In this approach, no statistical assumptions are employed. The problem is formulated in such a way that from the very beginning one solves a traditional nuclear problem (shell model with Woods–Saxon potential). On the basis of its solution the coupled-channel method is developed, and calculations by it yield the energies, widths, and wave functions of all nuclear states ("resonance states," including both bound and decay states), and also the reaction cross section and the S matrix. The approximations used to derive the equations in Ref. 1 are as follows:

a) only the proton and neutron decay channels are taken into account;

b) the state of the residual nucleus with $A-1$ nucleons is stable.

In numerical calculations, two approximations are used:

a) a density-independent spin-exchange residual interaction of zero range;

b) the configuration space for the nuclei with both A and $A-1$ nucleons is truncated in the standard shell-model manner (i.e., for 1 p-shell nuclei a restriction is made to the configurations $1s_{1/2}$, $1p_{3/2}$, $1p_{1/2}$, $2s_{1/2}$, $1d_{5/2}$, $1d_{3/2}$).

Thus, the method generalizes the traditional shell model by including nucleon decay channels.

A solution of the Schrödinger equation $(H-E)\Psi=0$ is sought in the form

$$\Psi_E^{c(+)}=\sum_{i=1}^{M} b_E^c(i)\,\Phi_i+\sum_{c'=1}^{\Lambda}\int_{\varepsilon_{c'}}^{\infty} dE' a_E^c(E';\,c')\,\chi_{E'}^{c'}, \qquad (1)$$

where the first term is the shell wave function with all A particles bound, whereas the second term corresponds to the channel wave functions with $A-1$ particles in a bound state and one particle in a scattering state. The index c denotes the channel and ε_c the threshold energy for channel c. To find the wave function Ψ_E^c, the total function space is decomposed into the two subspaces of the states of the continuum and discrete spectrum by means of projection operators P and Q. In contrast to Feshbach's traditional method,[4] the technique of projection operators is used here not to separate the part of the problem in which we are interested from the other parts with a view to using different approximations for the different parts, but rather to employ approximations of the same kind (truncation of both the number of configurations and the number of channels) for functions that have quite different mathematical properties. Therefore, the decomposition of the space of functions into two subspaces in the shell model in the continuum differs from the analogous decomposition in Feshbach's theory. In the shell model in the continuum, the Q space contains the wave functions of all the discrete states, whereas the P space includes wave functions corresponding to one particle in a scattering state and the remainder in discrete states. If there is a narrow single-particle resonance in the continuum, it is included in the subset of discrete states up to the cutoff radius R_{cut}, whereas the remaining part is put in the P space. By means of such a procedure the Q space is constructed from a subset of discrete states analogous to those used in traditional shell-model calculations for bound states. This subspace contains the part of the total wave function that has a large amplitude within the nucleus. In the model space thus chosen, the condition $P+Q=1$ holds, and also the condition of orthogonality between the two subspaces if there is a certain renormalization of the wave functions.

Single-Particle Spectrum

The Hamiltonian describing the system of A nucleons is taken in the form

$$H=H_0+V, \qquad (2)$$

where V is the residual interaction. The unperturbed shell-model Hamiltonian H_0 is a sum of single-particle operators:

$$H_0=\sum_i h_0(r_i). \qquad (3)$$

The operator h_0, which depends on the coordinate of one nucleon, generates the spectrum of single-particle states in a shell-model potential of finite depth. These single -particle states form a basis by means of which the total wave function is constructed.

Assuming that the shell-model potential is spherically symmetric, we can classify the wave functions φ_α by means of the total and orbital angular momenta l and j:.

$$\varphi_\alpha(r)=i^{l_\alpha}Y_{l_\alpha j_\alpha m_\alpha}(\Omega)\,\chi_{\tau_\alpha}\frac{1}{r}u_{e_\alpha\tau_\alpha l_\alpha j_\alpha}(r). \qquad (4)$$

The index α identifies the quantum numbers l_α and j_α the projection m_α of the total angular momentum, the third component of the isospin τ, and also the energy e_α. The function Y_{ljm} is obtained by adding a spherical function to the nucleon spin function. The function χ_τ is an eigenfunction of the third component of the isospin operator with eigenvalue τ. In accordance with (4), we represent the single-particle operator h_0 in the form

$$h_0(r)=\sum_{\tau ljm} i^l Y_{ljm}(\Omega)\,\chi_\tau\frac{1}{r}h_{\tau lj}(r)\,r\int d\Omega' i^{-l}Y_{ljm}^{\dagger}(\Omega')\,\chi_\tau. \qquad (5)$$

Here, the operator $h_{\tau lj}$ depends only on the radial coordinate:

$$h_{\tau lj}(r)=\frac{\hbar^2}{2m_r}\left(-\frac{d}{dr^2}+\frac{l(l+1)}{r^2}\right)+V_{\tau lj}(r). \qquad (6)$$

It contains the finite-depth shell-model potential $V_{\tau lj}$, which depends in general on the quantum numbers of the states. The parameters of this potential are chosen in such a way that the eigenvalues of the Hamiltonian $h_{\tau lj}$ reproduce the known experimental single-particle energies. The reduced nucleon mass is $m_r=(1-1/A)m_{\text{nuc}}$.

Using the truncation method proposed by Wang and Shakin[3] for single-particle resonances, we can represent the discrete states in the form

$$u_{n\tau lj}(r)=\tilde{u}_{n\tau lj}(r),\quad n=0,\ 1,\ \ldots,\ M-1: \qquad (7a)$$

$$u_{M\tau lj}(r) = N_{M\tau lj}\vartheta(R_{\text{cut}} - r)\,\tilde{u}_{\varepsilon_r\tau lj}(r) + \sum_{n=1}^{M-1} N_{n\tau lj}\tilde{u}_{n\tau lj}(r). \tag{7b}$$

The functions $\tilde{u}$ are solutions of the radial Schrödinger equation with the single-particle operator $h_{\tau lj}(r)$:

$$(E_{n\tau lj} - h_{\tau lj}(r))\,\tilde{u}_{n\tau lj}(r) = 0,\ n = 0,\ 1,\ \ldots,\ M-1; \tag{8}$$

$$(\varepsilon - h_{\tau lj}(r))\,\tilde{u}_{\varepsilon\tau lj}(r) = 0,\quad \varepsilon > 0. \tag{9}$$

The M discrete solutions correspond to energies $e = E_{n\tau lj} < 0$, and the index e is replaced by the number n of nodes of the wave function. The continuum solutions are determined by the energy eigenvalues $e = \varepsilon > 0$. The step function $\theta(R_{\text{cut}} - r)$ cuts off the single particle function $\tilde{u}_{\varepsilon\tau lj}$ at the point $r = R_{\text{cut}}$. The energy ε_r lies near a resonance energy: $u_{\varepsilon_r\tau lj} \equiv u_{M\tau lj}$. The constants $N_{n\tau lj}$ $(n = 0,1,\ldots,M)$ ensure the normalization and mutual orthogonality of the functions (7). The state defined in (7b) is called a quasibound single-particle state.

In accordance with the definition of the discrete states (7) we obtain for the continuum the equation

$$[\varepsilon - (1 - q_{\tau lj})\,h_{\tau lj}(r)\,(1 - q_{\tau lj})]\,u_{\varepsilon\tau lj}(r) = 0, \tag{10}$$

in which the projection operator

$$q_{\tau lj} = \sum_{n=0}^{M} u_{n\tau lj}(r) \int dr' u_{n\tau lj}(r') \tag{11}$$

projects onto the single-particle states. Equation (10) ensures orthogonality between the discrete and continuum states. Thus, the single-particle spectrum can be chosen in such a way as to satisfy the orthogonality conditions

$$\int dr u_{n\tau lj}(r)\,u_{n'\tau lj}(r) = \delta_{nn'}; \tag{12}$$

$$\int dr u_{n\tau lj}(r)\,u_{\varepsilon\tau lj}(r) = 0; \tag{13}$$

$$\int dr u_{\varepsilon\tau lj}(r)\,u_{\varepsilon'\tau lj}(r) = \delta(\varepsilon - \varepsilon') \tag{14}$$

and the completeness condition

$$\sum_{n=0}^{M} u_{n\tau lj}(r)\,u_{n\tau lj}(r') + \int_0^\infty d\varepsilon u_{\varepsilon\tau lj}(r)\,u_{\varepsilon\tau lj}(r') = \delta(r - r') \tag{15}$$

Since the function (7b) and the continuum functions are not eigenfunctions of the single-particle operator h, we can define a new operator $\bar{h}$, which generates the complete single-particle spectrum:

$$\bar{h}_{\tau lj}(r) = \sum_{n=0}^{M} u_{n\tau lj}(r)\,E_{n\tau lj} \int dr' u_{n\tau lj}(r') + (1 - q_{\tau lj})\,h_{\tau lj}(r)\,(1 - q_{\tau lj}). \tag{16}$$

The Hamiltonian $\bar{H}_0$ of the complete system is determined by Eqs. (3) and (7), in which the operators $h_{\tau lj}$. must be replaced by the operators $\bar{h}_{\tau lj}$.

Basic Equations

The Schrödinger equation $H\Psi = E\Psi$ with discrete and continuum states is solved as follows.

1. Solution of the standard shell-model problem with Woods–Saxon potential:

$$(E_R^{SM} - H_{QQ})\,\Phi_R = 0, \tag{17}$$

where $H_{QQ} = QHQ$. The operator

$$Q = \sum_R |\Phi_R\rangle\langle\Phi_R| \tag{18}$$

projects onto the subspace of discrete states. This subspace corresponds to the function space of the standard shell model by virtue of the use of the truncation technique for the description of narrow single-particle resonances. The states described by the functions Φ_R and the eigenvalues E_R^{SM} of the operator H_{QQ} are called quasibound states embedded in the continuum (QBSEC). In such states, all nucleons occupy bound or quasibound single-particle orbits. The QBSEC states correspond to the states obtained in the standard shell model.

2. Solution of the equations for the coupled channels:

$$(E^{(+)} - H_{PP})\,\xi_E^{c(+)} = 0 \tag{19}$$

with incident wave in the entrance channel and outgoing waves in all channels as boundary conditions. Here $H_{PP} \equiv PHP$. The operator

$$P = \sum_c \int_{\varepsilon_c}^{\infty} dE |\xi_E^{c(+)}\rangle\langle\xi_E^{c(+)}| \tag{20}$$

projects onto the subspace with one particle in the continuum and the remainder in discrete states (c channels). The threshold energies are denoted by ε_c. In numerical calculations, the operator P is represented by

$$P = 1 - Q, \tag{21}$$

by means of which the given configuration space is defined.

3. Solution of the equations for the coupled channels with a source:

$$(E^{(+)} - H_{PP})\,\omega_R^{(+)} = H_{PQ}\Phi_R, \tag{22}$$

where $H_{PQ} \equiv PHQ$. The source describes coupling of the two subspaces.

The solution Ψ is expressed in terms of the three functions Φ_R, $\xi_E^{c(+)}$, and $\omega_R^{(+)}$:

$$\Psi_E^{c(+)} = \xi_E^{c(+)} + \sum_{R,R'} (\Phi_R + \omega_R^{(+)})\,\frac{1}{E - M_{RR'}}\langle\Phi_{R'}|H_{QP}|\xi_E^{c(+)}\rangle. \tag{23}$$

Here, $M_{RR'}$ are the matrix elements

$$M_{RR'} = \sum_c \int_{\varepsilon_c}^{\infty} dE' \langle\Phi_R|H|\Phi_{R'} + \omega_{R'}^{(+)}\rangle \tag{24}$$

of the operator

$$H_{QQ}^{\text{eff}} = H_{QQ} + H_{QP}G_P^{(+)}H_{PQ}. \tag{25}$$

The operator H_{QQ}^{eff} is the part of the Hamiltonian that arises effectively in the Q space when the continuum is taken into account. The Green's function $G_P^{(+)} = P(E^+ - H_{PP})^{-1}P$ describes the motion of the particle in the P space.

The eigenfunctions

$$\tilde{\Phi}_R^{(+)} = \sum_{R'} \alpha_{RR'}^{(+)}\Phi_{R'} \tag{26}$$

and the eigenvalues $\tilde{E}_R - (i/2)\tilde{\Gamma}_R$ of the Hamiltonian H_{QQ}^{eff} determine the wave functions, energies

Numerical calculations in the framework of the shell model in the continuum are made using zero-range forces:

$$V(1, 2) = V_0 (a + bP_{12}^{\sigma}) \delta (\mathbf{r}_1 - \mathbf{r}_2), \quad (52)$$

where P_{12}^{σ} is a spin–exchange operator. In this case, the channel-coupling equations for the radial wave functions $\xi_c^{(J)}(r)$ have the form[1]

$$(E - E_t - h_c)\,\xi_c^{(J)}(r) - \sum_{c'} V_{cc'}^{(J)} \xi_{c'}^{(J)}(r) = -q_c (h_c \xi_c^{(J)}(r) + \sum_{c'} V_{cc'}^{(J)}(r)\,\xi_{c'}^{(J)}(r)). \quad (53)$$

In deriving (53), we have used the relation $q_c \xi_c^{(J)} = 0$, where q_c is defined in (11). It is obvious that the solutions of Eq. (53) also satisfy this condition.

The operator q_c in (53) ensures fulfillment of the Pauli principle for the many-particle function Ψ. If we compare (53) with the original equation (19), writing it formally as

$$\sum_{c'} (E\delta_{cc'} - H_{cc'})\,\xi_{c'}^{(J)} = -\sum_{c'c''} Q_{cc'} H_{c'c''} \xi_{c''}^{(J)}, \quad (54)$$

we readily see that the operator Q is diagonal in the channel representation and has the form:

$$Q_{cc'} = \delta_{cc'} q_c. \quad (55)$$

Equation (22) is solved by functions $\omega_R^{(+)}$ describing the tails of resonance wave functions. Using the formalism of the coupled-channel method, we can represent (22) in the form

$$\sum_{c'} (E\delta_{cc'} - H_{cc'})\,\omega_{c'}^{(R)} = w_c^{(R)} - q_c \left(\sum_{c'} H_{cc'} \omega_{c'}^{(R)} + w_c^{(R)}\right), \quad (56)$$

if we use the relation (55). The channel wave functions $\omega_c^{(R)}(r)$ are determined in accordance with (51). Asymptotically, they behave as purely outgoing waves and are generated by the sources $\omega_c^{(R)}$, which arise from the interaction H_{PQ}, the coupling of the discrete spectrum to the continuum.

The projection of the quasibound states embedded in the continuum Φ_R onto channel c can be expressed as follows:

$$\Phi_{R,c}^{(J)} = \sum_{n=0}^{M} S_{n,c}^{(R)} u_{n\tau lj}(r)\,|t), \quad (57)$$

where

$$S_{n,c}^{(R)} = \sum_{M_t m} \begin{pmatrix} I_t\ j \\ M_t m \end{pmatrix} \Big| \begin{matrix} J \\ M \end{matrix} \Big) (t|a_{n\tau ljm}|\Phi_R\rangle \quad (58)$$

is the spectroscopic amplitude for the single-particle state $n\tau lj$. The relations (57) and (58) for the discrete state Φ_R are analogous to Eq. (51) for the continuum state ξ. The source terms $\omega_c^{(R)}$ can be calculated using the channel wave functions ξ_c^J and $\Phi_{R,c}^J$.

It now remains to solve (54) and (56) numerically. Using (11), we can represent both equations in the form

$$\sum_{c'} (E\delta_{cc'} - H_{cc'})\,\zeta_{c'}(r) = I_c$$

$$-\sum_{n=0}^{M} u_{n\tau lj}(r) \int dr' u_{n\tau lj}(r') \left[I_c(r') + \sum_{c'} H_{cc'} \zeta_{c'}(r') \right]. \quad (59)$$

Here, ζ is a function of ω in Eq. (56) and a function of ξ in (54), and $I_c = w_c^{(R)}$ for (56) and $I_c = 0$ for (54). Equations (59) form a system of coupled differential equations with an inhomogeneous term on the right-hand side that is a linear combination of I_c and $u_{n\tau lj}$. The weight coefficients are integrals containing the solutions ζ_c. The solutions ζ_c can be found numerically as superpositions of two types of solutions, one of which satisfies the system of equations without the term containing the operator q but satisfying the same boundary conditions as are imposed on τ_c, namely, outgoing waves in all channels and, for the case $I_c = 0$, an incoming wave in the entrance channel.

If instead of (19) we solve (34), then it must also be rewritten in the form (59) with an inhomogeneous term on the right-hand side.

Details relating to the solution of the equations for the coupled channels can be found in Ref. 1.

2. INVESTIGATION OF NUCLEAR STRUCTURE IN THE FRAMEWORK OF THE SHELL MODEL IN THE CONTINUUM

Energies and Widths of Nuclear States

The shell model in the continuum is a generalization of the traditional shell model by the inclusion of a set of basis functions of continuum states. The subspace Q in this model corresponds to the function space employed in standard shell-model calculations. All nucleons occupy bound and quasibound states. The QBSEC states are discrete states of the continuous spectrum. The eigenvalues of the Hamiltonian H_{QQ} are real because this operator is Hermitian. They are the energies E_R^{SM} of the QBSEC states, and the functions corresponding to them are eigenfunctions of H_{QQ}. Thus, the results obtained by solving (17) are the results of traditional shell-model calculations with the Woods–Saxon potential. The QBSEC states are the states of the shell model.

The coupling of the nuclear states to the continuum is described by the operator H_{QQ}^{eff}, defined in (25). This operator is non-Hermitian for states above the threshold for emission of one particle. It is Hermitian only when the energy is below the lowest threshold for emission of a particle, and also in the limit $E \to \infty$. Thus, the operator H_{QQ}^{eff} is Hermitian for bound states and non-Hermitian for decay states. Its eigenvalues are real for bound states and complex for decay states. They describe, therefore, not only the energies but also the lifetimes of the states.

The eigenstates of the operator H_{QQ}^{eff},

$$H_{QQ}^{\text{eff}} \tilde{\Phi}_R = \left(\tilde{E}_R - \frac{i}{2}\tilde{\Gamma}_R\right)\tilde{\Phi}_R, \quad (60)$$

depend on the energy because of the explicit energy dependence of the propagator $G_P^{(+)}$ (25). The energies E_R and widths Γ_R of the resonance states can be calculated by means of (27) and (28). Usually, (27) has a solution lying in the neighborhood of the shell-model energy E_R^{SM} of the corresponding QBSEC. In the majority of cases, the shifts $\Delta E = E_R - E_R^{SM}$ are negative because the configuration space is increased by the addition of the P space. As a rule, the shifts and widths are of the same order.

As was established by Lemmer and Shakin,[5] Eq. (27) in the solution of such a problem can also have solutions at energies $E'_R = E_R$. In Ref. 1, in the framework of the shell

model in the continuum, it was shown in a numerical example that such additional solutions are associated with low-lying single-particle resonances, to which the truncation technique was not applied. Eliminating these resonances from the P space by means of the projection operator q (11), we obtain a curve $\tilde{E}_R(E)$ that has a smooth energy dependence and ensures a unique solution. This means that (27) and (28) have unique solutions if all wave functions with large amplitude within the nucleus are included in the Q space, and the contribution from the wave functions of the P space within the nuclei is small. This result shows once more that the Q space must be similar to the space of the standard shell model, for which the contribution from the wave functions within the nucleus is important, and not their asymptotic behavior. Therefore, to investigate properties of nuclear structure in the framework of the shell model in the continuum it is necessary to use the truncation technique for the single-particle resonances. Of course, the cross section of a nuclear reaction does not depend on the method of division of the complete space into two subspaces.

The diagonal matrix elements of the operator H_{QQ}^{eff} have the form

$$\langle\Phi_R|H_{QQ}^{\text{eff}}|\Phi_R\rangle = E_R^{SM} + \sum_c \int_{\varepsilon_c}^{\infty} dE' \langle\Phi_R|H|\xi_{E'}^c\rangle \frac{1}{E^{(+)}-E'} \times \langle\xi_{E'}^c|H|\Phi_R\rangle. \quad (61)$$

Their real part is given by

$$\tilde{E}_R^{(\text{iso})} = E_R^{SM} + \Delta\tilde{E}_R^{(\text{iso})}, \quad (62)$$

where

$$\Delta\tilde{E}_R^{(\text{iso})} = \sum_c \mathcal{P}\int_{\varepsilon_c}^{\infty} dE' \langle\Phi_R|H|\xi_{E'}^c\rangle \frac{1}{E-E'} \langle\xi_{E'}^c|H|\Phi_R\rangle, \quad (63)$$

and the imaginary part has the form

$$\frac{1}{2}\tilde{\Gamma}_R^{(\text{iso})} = \pi \sum_c \langle\Phi_R|H|\xi_E^c\rangle \langle\xi_E^c|H|\Phi_R\rangle. \quad (64)$$

The quantities

$$E_R^{(\text{iso})} = \tilde{E}_R^{(\text{iso})}(E = E_R); \quad (65)$$

$$\Gamma_R^{(\text{iso})} = \tilde{\Gamma}_R^{(\text{iso})}(E = E_R) \quad (66)$$

are the energy and width of an isolated resonance. Generally speaking, they differ from E_R and Γ_R through the influence of the external mixing described by the nondiagonal matrix elements $\langle\Phi_R|H_{QQ}^{\text{eff}}|\Phi_{R'}\rangle$ in (32). In traditional nuclear calculations, the external mixing is not taken into account. It cannot be fully taken into account by the introduction of an additional term into the residual interaction, since it has a many-particle nature, depending, for example, on the threshold for separation of particles.

It is well known[6] that any truncation of the function space can be formally compensated by the addition of an effective part to the Hamiltonian, i.e., by replacing H_{QQ} by an effective operator H_{QQ}^{eff}. Here, $Q\Psi$ is part of the function space taken into account explicitly, and $P\Psi$ is the part truncated. In our case, H_{QQ}^{eff} contains the effects of the influence of the continuum on the properties of the discrete state.

Wave Function of a Nuclear State

In accordance with (30) and (31), the wave function of the discrete nuclear state R is

$$\tilde{\Omega}_R^{(+)}(E = E_R) = \tilde{\Phi}_R^{(+)}(E = E_R) + \tilde{\omega}_R^{(+)}(E = E_R). \quad (67)$$

Here, $\tilde{\Phi}_R$ is an eigenfunction of H_{QQ}^{eff}, and $\tilde{\omega}_R$ is its continuation to the P space. The wave functions $\tilde{\Omega}_R$ are obtained directly. Their asymptotic behavior in the form of outgoing waves corresponds to the concept of a resonance state.[7] But this concept is meaningful only when the difference between $\tilde{\Omega}_R$ and $\tilde{\Phi}_R$ is negligibly small in the interior region, i.e., if the amplitude of the resonance wave function $\tilde{\Omega}_R$ within the nucleus is sufficiently large compared with the amplitude of the function $\tilde{\omega}_R$.[7] This condition is satisfied in the shell model in the continuum, since the functions ξ_E^c of the P space do not have large amplitudes within the nucleus by virtue of the truncation technique for the single-particle resonances. In the shell model in the continuum, the expectation value of A is calculated by means of the wave functions $\tilde{\Phi}_R$:

$$\langle A\rangle = \langle\tilde{\Phi}_R|A|\tilde{\Phi}_R\rangle / \langle\tilde{\Phi}_R|\tilde{\Phi}_R\rangle. \quad (68)$$

The term $\tilde{\omega}_R$ in (67) describes the surface properties of the nucleus. It explicitly contains a coupling to both the open and closed channels and characterizes singularities of the state. The virtual particles associated with closed channels form the nuclear surface. The appearance of nucleons in the nuclear surface in the form of individual particles or in the form of clusters depends on the position of the thresholds for the emission of a nucleon or, for example, an α particle. If the thresholds for α decay are the lowest, one must expect clustering of the nucleons in the nuclear surface. Individual nucleons will appear in the surface of the nucleus if all the cluster thresholds lie above the single-nucleon thresholds. A surface term arises not only for states lying above the particle-emission thresholds but also for states in which all channels are closed.

Despite the apparent similarity, the concept of a resonance state in the shell model in the continuum is different from the one formulated by Mahaux and Weidenmüller[2] in their shell-model approach to nuclear reactions. In their theory, as was shown in Ref. 5, the energies E_R and widths Γ_R are not determined uniquely by (27) and (28). Only the use of the truncation technique for the single-particle resonances[3] ensures uniqueness of the solution. Therefore, the isolated resonances observed in the cross section correspond to the QBSEC states introduced by Barz *et al.*[1] and not, in general, to bound states embedded in the continuum (BSEC), which were determined in Ref. 2 by Mahaux and Weidenmüller.

The concept of an isolated resonance state R in the shell model in the continuum corresponds to its definition in R-matrix theory,[8] since the QBSEC states are states of the shell model that takes into account the main contribution from the single particle resonances within the nucleus. Thus, in the case of an isolated resonance the calculations in the shell model in the continuum are in general agreement with the results of numerous calculations in the framework of the standard shell model.

In the approach considered here, no statistical assump-

tions are made. Thus, the shell model in the continuum also applies in the case of overlapping resonances, i.e., when the cross section is an interference pattern.

The correlations between levels are determined by two factors, the relative importance of which depends on the degree of overlapping of the levels: 1) the configuration or internal mixing, which is calculated in all nuclear -structure models; 2) external mixing, due to coupling of each state to the continuum. The QBSEC states contain only internal mixing, described by H_{QQ}. The real nuclear states contain an additional external mixing described by the nondiagonal matrix elements of (32). The external mixing is important at higher excitation energies, when the resonance states overlap. The difference between $\widetilde{\Phi}_R$ and Φ_R and between the eigenvalues of H_{QQ}^{eff} and its diagonal matrix elements $\langle \Phi_R | H_{QQ}^{\text{eff}} | \Phi_R \rangle$ reflects the effects of the external mixing on the wave function and, accordingly, on the energy and width of the resonance state.

We must point out the difference between the definition of external mixing here and the one used in the literature. Robson[9] defines external mixing as the coupling of states with different isospins through the continuum. In Ref. 10, internal and external mixing of states with different isospins was calculated in the $p_{3/2}$ isobar analog resonance in ^{41}K. In Ref. 11, Harney *et al.* estimated the contribution from external mixing to the isospin-mixing matrix elements, using statistical assumptions. In all the quoted studies it was assumed that, like internal mixing, external mixing leads to fragmentation, i.e., no allowance was made for the signs of the external and internal mixing.

In the present paper, the concept of external mixing has a more general meaning. It is defined on the basis of a dynamical model (the shell model in the continuum) without any statistical assumptions. Thus, there are here no restrictions to isospin matrix elements or to the case of weak absorption in all channels. Moreover, the sign of the external mixing is not assumed from the beginning to be the same as that of the interior mixing but is calculated in the framework of the model, i.e., the interior and external mixing are described in a unified manner.

Partial Widths

The partial width $\Gamma_{R,c}$ of the decay state R is defined as $\Gamma_{R,c} = |\gamma_{R,c}|^2$, where

$$\gamma_{R,c} = (2\pi)^{1/2} \langle \chi_E^{c(-)} | V | \widetilde{\Omega}_R^{(+)} \rangle |_{E=E_R}. \tag{69}$$

Here, $\widetilde{\Omega}_R^{(+)}$ is the wave function of the decay state (67). The function χ_E^c describes the final state and is determined by Eqs. (1), (10), and (46):

$$\chi_F^c = u_{\varepsilon_\tau lj} | t). \tag{70}$$

It differs from the function ξ_E^c by absence of the channel-coupling contribution due to the residual interaction V.

Using (22) and (30), we obtain

$$\langle \chi_E^{c(-)} | V | \widetilde{\Omega}_R^{(+)} \rangle = \langle \chi_E^{c(-)} | V (1 + G_P^{(+)} V) | \widetilde{\Phi}_R^{(+)} \rangle. \tag{71}$$

It follows from (19) and (11) that

$$\xi_E^{c(+)} = \chi_R^{c(+)} + G_P^{(+)} V \chi_E^{c(+)}. \tag{72}$$

Using these relations in (71), we obtain

$$\langle \chi_E^{c(-)} | V | \widetilde{\Omega}_R^{(+)} \rangle = \langle \xi_E^{c(-)} | V | \widetilde{\Phi}_R^{(+)} \rangle. \tag{73}$$

Thus, the matrix element (69) can be rewritten in the form

$$\gamma_{R,c} = (2\pi)^{1/2} \langle \xi_E^{c(-)} | H | \widetilde{\Phi}_R^{(+)} \rangle_{E=E_R}, \tag{74}$$

in the derivation of which we have used the relation

$$\langle \xi_E^{c(-)} | H_0 | \widetilde{\Phi}_R^{(+)} \rangle = 0.$$

For isolated resonance states, the total width is determined by (64) and (66). Using (74) for the amplitude of the partial width, we obtain

$$\Gamma_R^{(\text{iso})} = \sum_c \Gamma_{R,c}^{(\text{iso})}, \tag{75}$$

i.e., the decay width $\Gamma_R^{(\text{iso})}$ is the sum of the partial widths $\Gamma_{R,c}^{(\text{iso})}$.

In standard nuclear-structure calculations the total widths are not determined directly, since the calculations are made with an Hermitian Hamiltonian. Therefore, to determine the total width the relation (75) is used always. In the shell model in the continuum, the relation (75) is obtained by direct diagonalization of the non-Hermitian Hamiltonian H_{QQ}^{eff}, and, moreover, both sides in (75) are calculated. Thus, the relation (75) can be used to verify the results. We emphasize that (75) holds only for isolated resonances.

The diagonal matrix elements H_{QQ}^{eff} can be expressed as

$$E - \widetilde{E}_R + \frac{i}{2} \widetilde{\Gamma}_R = \sum_{ij} \alpha_{Ri} \alpha_{Rj} \langle \Phi_i | H_{QQ}^{\text{eff}} | \Phi_j \rangle \delta_{RR'}, \tag{76}$$

if we use the representation (26) for the wave function $\widetilde{\Phi}_R$. Multiplying (76) by $\alpha_{Rk}^* \alpha_{R',k}$ and summing over R' and k, we obtain:

$$\left(E - \widetilde{E}_R + \frac{i}{2} \widetilde{\Gamma}_R \right) \sum_k |\alpha_{Rk}|^2 = \sum_{ij} \alpha_{Ri} \alpha_{Rj}^* \langle \Phi_i | H_{QQ}^{\text{eff}} | \Phi_j \rangle, \tag{77}$$

bearing in mind that $\Sigma_R \alpha_{R,k} \alpha_{R,j} = \delta_{kj}$. The real part of the right-hand side of (77) has the form:

$$\text{Re} \left(\sum_{ij} \alpha_{Ri} \alpha_{Rj}^* \langle \Phi_i | H_{QQ}^{\text{eff}} | \Phi_j \rangle \right) = \sum_i |\alpha_{Ri}|^2 E_i^{SM} + \sum_c \mathcal{P} \int_{\varepsilon_c}^{\infty} dE' \frac{\langle \widetilde{\Phi}_R^* | H | \xi_{E'}^c \rangle \langle \xi_{E'}^c | H | \widetilde{\Phi}_R^* \rangle}{E - E'}, \tag{78}$$

and the imaginary part is

$$\text{Im} \left(\sum_{ij} \alpha_{Ri} \alpha_{Rj}^* \langle \Phi_i | H_{QQ}^{\text{eff}} | \Phi_j \rangle \right) = \pi \sum_c \langle \widetilde{\Phi}_R^* | H | \xi_E^c \rangle \langle \xi_E^c | H | \widetilde{\Phi}_R^* \rangle. \tag{79}$$

Using (74) for the amplitude of the partial width, we find from (77) and (79) that

$$\widetilde{\Gamma}_R \sum_k |\alpha_{Rk}|^2 = \sum_c \widetilde{\Gamma}_{R,c}. \tag{80}$$

Here, the energy-dependent matrix elements (73) are denoted as $(2\pi)^{-1/2} \widetilde{\gamma}_{R,c}$ or $(2\pi)^{-1/2} \widetilde{\Gamma}_{R,c}^{1/2}$. The relation (80) is very general.[2] It is not a consequence of the special definition of the wave functions Φ_R and ξ_E^c used here. Bearing in mind that $\Sigma_R |\alpha_{Rk}|^2 > 1$, and using also the relation (28), we obtain

$$\Gamma_R \leqslant \sum_c \Gamma_{R,c}. \tag{81}$$

The equality sign holds here only for isolated resonance states, i.e., in the cases when the external mixing disappears.

In accordance with (81), the sum of the absolute magnitudes of the partial widths for a nonisolated resonance state is greater than its total width. Therefore, it is difficult to extract information about the partial widths from measurements of lifetimes. Indeed, there were, for example, problems in interpreting lifetime data in ^{239}U, in which it was found[12–14] that the lifetime is effectively independent of the excitation energy at a high level density. This contradicted theoretical estimates obtained for the neutron partial widths on the basis of theories with statistical assumptions. Similar problems also arose in the interpretation of lifetime data for nuclei of medium mass. In proton scattering by Ni, for example, the experimentally determined mean lifetime of the compound nucleus was found to be much longer than that predicted by purely statistical theories.[15]

Usually, the partial widths $\Gamma_{R,c}$ are calculated by means of the overlap integrals of the nuclear wave functions before and after decay. In accordance with (69) and (67), $\gamma_{R,c}$ for an isolated state R consists of two parts, proportional to

$$a_1 = \langle \chi_E^{c(-)} | V | \Phi_R \rangle \tag{82}$$

and

$$a_2 = \langle \chi_E^{c(-)} | V | \omega_R^{(+)} \rangle. \tag{83}$$

Projecting the wave function Φ_R onto channel c, i.e., using Eqs. (57) and (58), we obtain

$$a_1 \approx \sum_{n=0}^{M} S_{n,c}^{(R)} \langle u_{\varepsilon\tau lj t} | V | u_{n\tau lj t} \rangle. \tag{84}$$

Here, $S_{n,c}^{(R)}$ is the spectroscopic amplitude for the single-particle state $n\tau lj$, and the matrix element describes penetration of a particle from the interior part of the nucleus to the exterior part. The relation (84) justifies the factorization approximation for a_1 that is generally used to calculate the partial width. But a_2, which has the form

$$a_2 = \sum_{c'} \int_{\varepsilon_{c'}}^{\infty} dE' \langle \chi_E^{c(-)} | V | \xi_{E'}^{c'(+)} \rangle \frac{1}{E^+ - E'} \langle \xi_{E'}^{c'(+)} | H | \Phi_R \rangle, \tag{85}$$

does not factorize.

Therefore, for $a_1 \gg a_2$ the factorization method is justified for calculating the partial width. But for transitions with small spectroscopic factors, when a_1 and a_2 are of the same order, the partial width cannot be factorized in the form of a spectroscopic factor and a penetrability factor. In these cases, the problem of obtaining the partial widths from the spectroscopic factors is nontrivial. It is necessary to take into account the channel coupling for the continuum states like the configuration mixing of discrete states in accordance with the representation (74) for the partial width.[16]

We consider below an example in which the factorization assumption is not satisfied. It is the excitation of the isospin-forbidden analog resonance $J^\pi = 3/2^-$, $T = 3/2$ at 15.1 MeV in the mirror nuclei ^{13}N and ^{13}C (Fig. 1). In the calculations of Ref. 17, isospin mixing was taken into account by means of perturbation theory. It was shown that

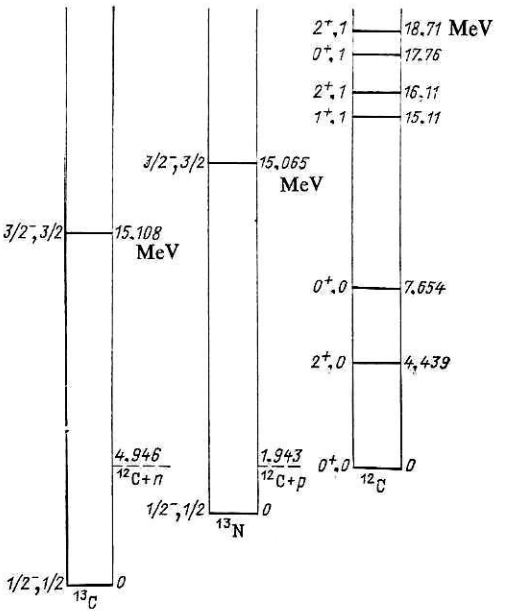

FIG. 1. Level schemes of the nuclei ^{13}C, ^{13}N, and ^{12}C.

internal mixing alone does not explain the observed decay widths. Only when an isotensor component in the charge-dependent residual interaction is taken into account do the calculated decay widths agree with the experimental ones. But in the investigations of Marrs *et al.*[18] of mirror Ml transitions in $A = 13$ nuclei it was shown that there are no indications of the presence of an isotensor component in the electromagnetic interaction. Thus, there was no understanding of the reason why the charge-dependent matrix elements are large for the $3/2^-$, 3/2 resonance at 15.1 MeV in the ^{13}C and ^{13}N nuclei.

In Ref. 19, the shell model in the continuum was used for numerical calculations for the ^{12}C + p and ^{12}C + n reactions, and excitations of two resonance states in the mirror nuclei at the energy 15.1 MeV were considered.

The shell-model calculations for the nuclei ^{13}N, ^{13}C, and ^{12}C are done in the complete $(1p_{3/2}, 1p_{1/2})$ configuration space. The parameters of the nucleon–nucleon interaction (52) for $V_0 = -650$ MeV/F^3 were taken, and three different sets were used for a and b. The parameters of the Woods–Saxon potential are analogous to those for the systems with $A = 16$. They were taken to be the same for protons and neutrons to simplify the discussion of the results: $V(l=0) = 56.36$ MeV, $V(l=1) = 57.67$ MeV, $V(l=2) = 54.65$ MeV and $V_{ls}(l=1) = 9.76$ MeV, $V_{ls}(l=2) = 5.27$ MeV. With these parameters, the Q values calculated without coupling to the continuum and also the level scheme are reproduced fairly well.[19] Internal isospin mixing was allowed both in the calculation of the QBSEC states and in the calculation of the states of the target nucleus. Calculations with coupled channels were made with all eight $3/2^-$ resonances for the systems with $A = 13$ and with six channels corresponding to the 0^+ states at 0, 7.66, and 17.77 MeV and the 2^+ states at 4.41, 16.11, and 18.80 MeV. After the choice of the nucleon–nucleon interaction, the size of the configuration space, and the number of channels, no other approximations were made

TABLE I. Width $\Gamma_R^{(\mathrm{iso})}$ of the $3/2^-$, 3/2 resonance state at 15.1 MeV in the ^{13}N nucleus.

Number of channels	Corresponding states of ^{12}C						$\Gamma_R^{(\mathrm{iso})}$, keV
	$(0^+, 0)_1$	$(0^+, 0)_2$	$(0^+, 1)_1$	$(2^+, 0)_1$	$(2^+, 1)_1$	$(2^+, 1)_2$	
6	X	X	X	X	X	X	6.44
1	X	—	—	—	—	—	0,19
2	X	X	—	—	—	—	0.37
3	X	X	X	—	—	—	0.38
3	X	X	—	X	—	—	0,42
4	X	X	X	X	—	—	1,01
5	X	X	—	X	X	X	4.69

Note. "X" means that the corresponding state is taken into account and "—" indicates absence of the state in the calculation.

in the solution of the equations of the shell model in the continuum.

The numerical calculations show that both the internal and the external mixing of the nuclear compound states are weak.[19] This agrees with the results of Ref. 17. However, the widths Γ_R (28) obtained in the shell model in the continuum are not small. They are of the same order as the experimental values, although there was no explicit introduction of either an isotensor component or even a Coulomb term into the residual interaction. The width is not small because of the difference between the neutron and proton wave functions. To understand why the widths are large despite the small isospin mixing, the influence of channel coupling on the width $\Gamma_R^{(\mathrm{iso})}$ (66) was investigated. The results show that the coupling of the open isospin-forbidden channels to the closed but isospin-allowed states increases the width of the $3/2^-$, 3/2 level by at least an order of magnitude (Table I), although external mixing was not taken into account in the calculations. The extent to which the different channels influence the width $\Gamma_R^{(\mathrm{iso})}$ through the channel coupling depends on the degree of isospin purity and the structure of the corresponding nuclear states (Table I).

The reason why the channel coupling has a strong influence on the width $\Gamma_R^{(\mathrm{iso})} \approx |\gamma_{R, c_0}|^2$ in the considered case resides in the fact that a_1 (82) has a small value by virtue of the isospin selection rules. Therefore, the component a_2 in (83) cannot be ignored. Its value can be expressed in terms of the scattering wave function ξ_E^c. In this connection, it should be noted that from the point of view of the shell model in the continuum the channel coupling is not only a property of the considered reaction. It is also present in the asymptotic behavior ω_R of the wave function Ω_R of the resonance state. Thus, channel coupling is a property of the resonance state itself. This interpretation is in agreement with the conclusions from the experimental data, which indicate that the charge-dependent matrix element in the case of ^{16}O is determined by the properties of the resonance state.[20]

In the majority of partial-width calculations (see, for example, Ref. 17), the Pauli principle is not taken into account between the bound complex and the particle in the continuum. In Ref. 19, this approximation was investigated. It was shown that both the energies and the widths calculated with and without allowance for the Pauli principle differ appreciably. The discrepancy is particularly large when the widths are small, this being due to the selection rules with respect to the isospin variables. Finally, in calculations with allowance for the Pauli principle the external mixing has a weak influence on the widths and energies of the resonance states, in contrast to the calculations that do not take into account this principle. This example illustrates that the widths of isolated resonance states can be calculated with good accuracy without allowance for external mixing if one takes into account correctly the completeness relation for the single-particle wave functions of the bound states and the scattering states, and also the channel coupling.

S matrix

The general expression for the S matrix is[2]

$$S_{cc'} = \exp(2i\delta_c)\,\delta_{cc'} - 2\pi i \langle \chi_E^{c'(-)} | V | \Psi_E^{c(+)} \rangle. \tag{86}$$

Using (29), we can obtain[21]

$$S_{cc'} = S_{cc'}^{(1)} - S_{cc'}^{(2)}, \tag{87}$$

where

$$S_{cc'}^{(1)} = \exp(2i\delta_c)\,\delta_{cc'} - 2\pi i \langle \chi_E^{c'(-)} | V | \xi_E^{c(+)} \rangle \tag{88}$$

is a smooth function of the energy, and

$$S_{cc'}^{(2)} = 2\pi i \sum_R \langle \chi_E^{c'(-)} | V | \widetilde{\Omega}_R^{(+)} \rangle \frac{1}{E - \widetilde{E}_R + \frac{i}{2}\widetilde{\Gamma}_R} \langle \widetilde{\Phi}_R^{(-)} | V | \xi_E^{c(+)} \rangle \tag{89}$$

contains a contribution from the resonance states R. Using (73), we can rewrite the term $S_{cc'}^{(2)}$ in the form

$$S_{cc'}^{(2)} = 2\pi i \sum_R \langle \xi_E^{c'(-)} | V | \widetilde{\Phi}_R^{(+)} \rangle \frac{1}{E - \widetilde{E}_R + \frac{i}{2}\widetilde{\Gamma}_R} \langle \widetilde{\Phi}_R^{(-)} | V | \xi_E^{c(+)} \rangle. \tag{90}$$

Denoting the matrix element (73) by $(2\pi)^{-1/2}\widetilde{\Gamma}_{R,c}^{1/2} = (2\pi)^{-1/2}\widetilde{\gamma}_{R,c}$ in accordance with (69) and (74), we obtain

$$S_{cc'}^{(2)} = i \sum_R \frac{\widetilde{\gamma}_{R,c'}\widetilde{\gamma}_{R,c}}{E - \widetilde{E}_R + \frac{i}{2}\widetilde{\Gamma}_R}. \tag{91}$$

The expression for the S matrix through (87), (88), and (91) is obtained here without any approximations. It is valid for arbitrary energies and contains:

a) threshold effects, described by the functions $\widetilde{\Gamma}_R$, which we discuss below;

b) correlations of all the resonance states R; these arise from the configuration mixing, the channel coupling, and

the external mixing, which, being due to the residual interaction V, may lead to nonstatistical effects;

c) a restriction that follows from the unitarity condition for the S matrix for all resonances, including, by means of the truncation technique,[3] different types of giant resonances.

For isolated resonances, Eqs. (87), (88), and (91) can be approximated by means of the parametrized S matrix employed in standard theories of nuclear reactions. Then the energy-dependent functions $\widetilde{\gamma}_{R,c}$, $\widetilde{E}_R$, and $\widetilde{\Gamma}_R$ are replaced by the so-called parameters $|\gamma_{R,c}|$, E_R, and Γ_R. For overlapping resonances, this approximation is invalid, since the functions $\widetilde{\gamma}_{R,c}$ depend strongly on the energy, and the phases of the resonance states are correlated in accordance with the unitarity conditions. In this case, the resonance behavior of $S^{(2)}_{c,c'}$ is not determined by a sum of Breit–Wigner terms but has a more complicated form. Indeed, it follows from the unitarity condition of the S matrix that $\mathrm{Im}\,\widetilde{\gamma}_{R,c}$ is a function of all the denominators $(E-\widetilde{E}_R)^2+(1/4)\widetilde{\Gamma}^2_R$, and the relation

$$\Gamma_R < \sum_c |\gamma_{R,c}|^2$$

[see Eq. (81)] also holds, and this contradicts the assumptions generally employed to represent the cross section as a sum of isolated resonances.

It was shown some years ago[22] that for reactions with one open decay channel the S matrix can be parametrized identically in the different cases corresponding to different models of nuclear structure. The following two examples were considered[22]: first, when all levels are directly coupled to the entrance channel and, second, when only one of the levels is directly coupled to the entrance channel. Although the two cases are entirely different from the point of view of nuclear structure, experimentally they are indistinguishable if the analysis is done, as usual, by means of a parametrized S matrix. The reason for this is that there is a one-to-one correspondence between the parameters of the S matrix used for its representation under different physical conditions. In the case of all $M+1$ resonance states coupled to the entrance channel, the S matrix has the form

$$S=\exp(2i\delta)\frac{1-i\sum_{j=0}^{M}\frac{a_j^2}{E-\lambda_j}}{1+i\sum_{j=0}^{M}\frac{a_j^2}{E-\lambda_j}}, \tag{92}$$

while for $M+1$ resonance states of which only one is directly coupled to the entrance channel the S matrix has the form:

$$S=\exp(2i\delta)\frac{E-\varepsilon_0-\frac{i}{2}\Gamma^{\uparrow}-\sum_{m=1}^{M}\frac{v_m^2}{E-\varepsilon_m}}{E+\varepsilon_0+\frac{i}{2}\Gamma^{\uparrow}-\sum_{m=1}^{M}\frac{v_m^2}{E-\varepsilon_m}}. \tag{93}$$

In both cases, there are $2M+2$ parameters: a_j and λ_j in the first case, and also v_m, ε_m, ε_0, and $\Gamma\uparrow$ in the second. The realistic situation is between these two extreme cases.

Thus, it was shown in Ref. 22 that the presence of intermediate structure in the cross section of a nuclear reaction when only one decay channel is open does not contain indications of the existence of a doorway state. To explain the observed structure, calculations on the basis of a dynamical model are needed.

The shell model in the continuum is a dynamical model in which the structure of the nucleus and the cross sections of nuclear reactions are described in a unified manner—by means of Eqs. (87), (88), and (91) for the S matrix and Eqs. (27), (28), and (69) or (74) for $\widetilde{E}_R$, $\widetilde{\Gamma}_R$, and $\widetilde{\gamma}_{R,c}$. Intermediate structure can arise in the cross section because of either the presence of a short-lived nuclear state strongly coupled to at least one of the decay channels or fluctuations in the level density of long-lived nuclear states with the same spins and parity. In the second case, a short-lived nuclear state can be absent. Then the intermediate structure in the cross section is a nonstatistical effect due to the correlation of the long-lived, strongly overlapping states. The two extreme cases described by (92) and (93) may be different in the framework of the shell model in the continuum. Although the reaction cross section in both cases has the same form, the partial widths determined from the ratios of the cross sections for the different channels make it possible to distinguish these two extreme cases experimentally as well if more than one channel is open.

It follows from such an analysis of the S matrix that not every intermediate structure is due to a short-lived nuclear state strongly coupled to at least one of the decay channels. There are also intermediate structures associated with fluctuations in the density of levels having the same spin and parity. This result must be borne in mind in discussing the problem of resonances in heavy-ion reactions. The results of the numerical calculations for such problems are given in Refs. 23 and 24.

Threshold Effects and the Shapes of Isolated Resonances

The eigenvalues $\widetilde{E}_R-(1/2)\widetilde{\Gamma}_R$ of the operator H^{eff}_{QQ}, which determine the energies E_R and widths Γ_R of the resonant states R [see Eqs. (27) and (28)], depend on the energy. The imaginary part $(1/2)\widetilde{\Gamma}_R$ vanishes in the limit $E\to\varepsilon_1$, and also as $E\to\infty$, since the operator H^{eff}_{QQ} becomes Hermitian in accordance with (25) and (80). The quantity ε_1 is the lowest threshold of decay with emission of a particle. Therefore, $\widetilde{\Gamma}_R(E)$ increases with the energy at low energies but decreases at very high energies.

The partial width of an isolated resonance is determined by the matrix elements (69) or (74). In accordance with (61), the partial width vanishes as $E\to\varepsilon_{c'}$. Therefore, threshold effects are manifested in the function $\widetilde{\Gamma}_R(E)$, which increases when a new decay channel is opened. In accordance with (84), this increase depends on the magnitude of the spectroscopic factor of the state R with respect to the channel that becomes open.

Different types of threshold effects in nuclear reactions were considered in Ref. 25, in which the $^{15}\mathrm{N}+n$ and $^{16}\mathrm{O}+\gamma$ reactions were calculated using realistic wave functions. It was shown that the density of levels near the thresholds for particle emission hardly increases when a channel is

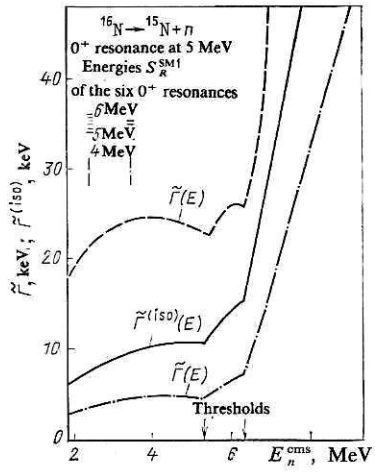

FIG. 2. The functions $\tilde{\Gamma}^{(iso)}(E)$ and $\tilde{\Gamma}(E)$ of the resonance state 1 with J^π, $T = 0^+$, 1 in ^{16}N. The sequence of inclusion of the remaining 0^+, 1 resonances is 1, 2, 3, 4, 5, 6 (broken curve); 3, 2, 1, 4, 5, 6 (chain curve).

opened. Moreover, the particle-emission thresholds are hardly affected by the presence or absence of correlations of the resonance levels established through the continuum. The only observable manifestations of the threshold effects are in the behavior of the functions $\tilde{\Gamma}_R$ and $\tilde{\Gamma}_R^{iso}$.

Figure 2 illustrates threshold effects in $\tilde{\Gamma}_R^{(iso)}(E)$. The calculations were made for six resonance levels with J^π, $T = 0^+$, 1 in the ^{16}N nucleus with $2p2h$ structure based on the shell-model configurations $(1p_{1/2})^{-2}[(1d_{5/2})^2$, $(1d_{5/2}, 2s_{1/2})$, $(1d_{5/2}, 1d_{3/2})$, $(2s_{1/2})^2]$, $(1p_{3/2})^{-1}$ $(1p_{1/2})^{-1}$ $[(d_{5/2})^2$, $(1d_{5/2}, 2s_{1/2})]$, $(1p_{3/2})^{-2}$ $(1d_{5/2})^2$. Allowance was made for four channels corresponding to the four lowest levels in ^{15}N. It was assumed that the states $1/2^-$ and $3/2^-$, which have negative parity, are hole $1p_{1/2^-}$ and $1p_{3/2^-}$ states. States with positive parity were obtained by diagonalizing the shell model Hamiltonian in the complete $1p2h$ configuration space with one particle in the $(1d_{5/2}, 2s_{1/2}, 1d_{3/2})$ shell and two holes in the $(1p_{3/2}, 1p_{1/2})$ shell. The threshold effects manifested in the functions $\tilde{\Gamma}_R^{(iso)}(E)$ also occur in $\tilde{\Gamma}_R(E)$ (Fig. 2). The difference between $\tilde{\Gamma}_R(E)$ and $\tilde{\Gamma}_R^{(iso)}(E)$ is due to the effects of external mixing with other resonances. The shell-model energies E_R^{SM} of the other five levels were chosen such that $E_1^{SM} < E_R^{SM}$ (broken curve) and $E_R^{SM} < E_1^{SM} < E_{R'}^{SM}$ (chain curve). Although it was assumed that resonance 1 does not overlap with the remaining five resonances, in both cases $\tilde{\Gamma}_1^{(iso)}$ and $\tilde{\Gamma}_1$ differed by about a factor of 2. In all the curves, the width increases when a new channel is opened.

The line shape of an isolated resonance is usually described by the Breit–Wigner formula

$$\sigma \sim \frac{\gamma_{R,c}\gamma_{R,c'}}{(E - E_R)^2 + \left(\frac{1}{2}\Gamma_R\right)^2}, \tag{94}$$

if interference with the direct part of the reaction can be ignored. Here, $\gamma_{R,c}$, E_R, and Γ_R are, respectively, the amplitude of the partial width, the energy, and the width of the resonance state R. It is assumed that they are constant parameters in the resonance region. Thus, the line shape is symmetric. Some deviations from symmetry arise because the energies ε_c are finite. Such deviations are taken into account in the Lorentz formula. In this formula Γ_R is also taken to be constant.

In the shell model in the continuum, in accordance with Eqs. (29), and also (27), (28), and (74), the quantities $\gamma_{R,c}$, E_R, and Γ_R in (94) are replaced by the energy-dependent functions $\tilde{\gamma}_{R,c}$, $\tilde{E}_R$, and $\tilde{\Gamma}_R$. This leads to correction , factors: $\tilde{E}_R(E)/E_R$ for the energy and $\tilde{\Gamma}_R(E)/\Gamma_R$ for the width in (94). Thus, the line shape is symmetric only when $\tilde{E}_R(E)$ and $\tilde{\Gamma}_R(E)$ are constant in the complete resonance region.

In the majority of cases, the functions $\tilde{\Gamma}_R$ increase with increasing energy of a giant resonance. For this reason, the majority of giant dipole resonances calculated in the shell model in the continuum for light nuclei decrease more slowly at high energies than at low. As an example, we consider the giant dipole resonance with J^π, $T = 1^-$, 1 in ^{16}O at 22.6 MeV, in the structure of which the $(1p_{3/2})^{-1}(1d_{5/2})$ configuration is dominant.[25] In this case, the direct part of the reaction is weak and, ignoring the interference with other resonances, the calculation can be made by the coupled channel method with one QBSEC state. The asymmetry of the line shape, i.e., the slower decrease at the higher energies, is due to the increase in $\tilde{\Gamma}_R$ with increasing energy. Another example is the J^π, $T = 1^-$, 1 resonance in ^{16}O at 19.6 MeV, whose structure is determined by the $(1p_{3/2})^{-1}(2s_{1/2})$ configuration.[25] Here, the asymmetry takes the form of a more rapid decrease of the right-hand arm of the resonance, this being explained by the decrease in $\tilde{\Gamma}_R$ with the energy. In the general case, the position of the maximum of the function $\tilde{\Gamma}_R(E)$ depends on the threshold energies of the channels whose reduced width is not small compared with the sum of the reduced width of all the channels.

The threshold behavior of the functions $\tilde{\Gamma}_R(E)$ may lead to strong deviations from the shape of the resonance lines predicted by the Breit–Wigner or Lorentz formulas. Figure 3 shows the energy dependence of the function $\tilde{\Gamma}_R$ for a 0^+

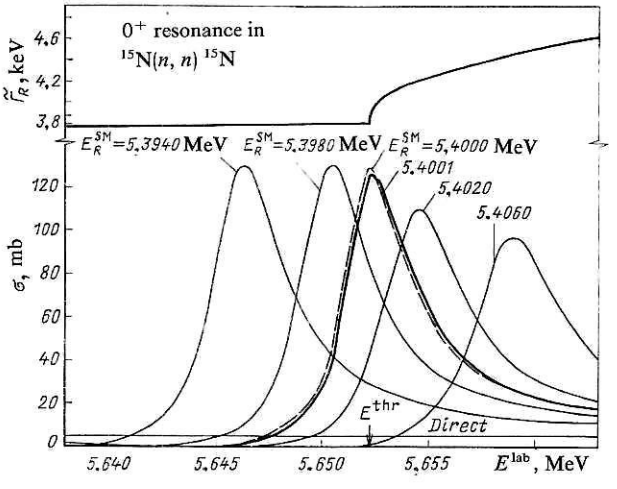

FIG. 3. Cross section for elastic neutron scattering by ^{15}N with one 0^+ resonance. The shell-model energy E_R^{SM} of the QBSEC state was varied. The function $\tilde{\Gamma}_R(E)$ is shown in the upper part of the figure; E^{thr} is the threshold energy of the $1/2^+$ neutron channel, and "Direct" denotes the direct part of the reaction.

resonance in the ^{16}N nucleus. The calculation was made in the same function space as in the case of the 0^+ resonance in Fig. 2. The calculations with channel coupling were made with only one QBSEC state in order to study the properties of this resonance in the absence of overlapping with other resonances. The function $\tilde{\Gamma}_R^{(\mathrm{iso})}(E)$ has an unusual behavior near the $1/2^+$ neutron threshold at $E^{\mathrm{thr}} = -5.299$ MeV, this behavior being due to the large reduced width of the 0^+ resonance relative to the channel which opens at $E^{\mathrm{cms}} = 5.299$ MeV. The partial widths corresponding to the elastic channel is approximately constant (3.8 keV) in the energy interval shown in Fig. 3. The cross section of elastic[15] $\mathrm{N} + n$ scattering with such a 0^+ resonance in ^{16}N is shown in the lower part of Fig. 3. The shell-model energy E_R^{SM} for the QBSEC state was chosen variously: $E_R < E^{\mathrm{thr}}$, $E_R > E^{\mathrm{thr}}$, and $E_R \approx E^{\mathrm{thr}}$. In the first case, the resonance is not completely symmetric, despite the fact that $\tilde{\Gamma}(E)$ is approximately constant. This is due to the effect of interference with the direct part of the reaction. In the second case, the resonance decreases more slowly at the higher energies because of the increase in $\tilde{\Gamma}(E)$. For $E_R \approx E^{\mathrm{thr}}$, a cusp rather than a resonance is observed in the cross section. For $E_R^{\mathrm{SM}} = 5.400$ MeV it is similar to the cusp observed experimentally in the $^7\mathrm{Li}(p,p)$ reaction.[27] It is also similar to the cusp obtained theoretically in Ref. 28 without particularization of the resonance structure, and also in Ref. 29, in which the three-particle problem for a single-particle resonance near a threshold was solved.

The results in Fig. 3 indicate that in real cases cusps appear very seldom, since they depend strongly on the barrier properties of the system and also on the nuclear structure of the resonance and the channel that opens up. Thus, a cusp is simply a resonance in the neighborhood of a threshold.

These examples illustrate the strong influence that the properties of the nuclear structure have on the cross section of nuclear reactions.

3. SYMMETRY BREAKING IN FINITE NUCLEI

Hamiltonian for a Finite Nucleus

Traditional nuclear-structure calculations are made with an Hermitian operator H_{QQ}. A certain part of the second term of the Hamiltonian H_{QQ}^{eff} (25) is taken into account by choosing the parameters in such a way that $E_R^{\mathrm{SM}} \approx E_R$ where E_R^{SM} is an eigenvalue of H_{QQ}, and E_Q an eigenvalue of H_{QQ}^{eff}. The matrix elements

$$\langle \tilde{\Phi}_R^{(+)} \mid H_{QQ}^{\mathrm{eff}} - H_{QQ} \mid \tilde{\Phi}_{R'}^{(+)} \rangle = \sum_c \int_{\varepsilon_c}^{\infty} dE' \, \langle \tilde{\Phi}_R^{(+)} \mid H \mid \xi_{E'}^{c(+)} \rangle \frac{1}{E^+ - E'} \langle \xi_{E'}^{c(+)} \mid H \mid \tilde{\Phi}_{E'}^{(+)} \rangle, \quad (95)$$

which explicitly contain the scattering wave functions ξ_E^c, including all the effects of the channel coupling, the matrix elements $\gamma_{R,c} = \langle \tilde{\Phi}_R \mid H \mid \xi_E^c \rangle$, and the threshold energies ε_c of the decay channels, have a many-particle nature. Therefore, it is impossible to take into account such matrix elements simply by introducing an additional term into the potential or into the residual interaction.

The matrix elements (95) characterize the properties of a finite nucleus. To a certain degree they violate the symmetry properties established theoretically in nuclear matter. For example the Coulomb forces form different threshold energies ε_c for the proton and neutron decay channels. Thus, the matrix elements (95) depend on the charge even when H_{QQ} is charge symmetric. The matrix elements (95) are also nonvanishing for bound states when all channels are closed. Therefore, symmetry-breaking effects hold for all states of a finite nucleus, including the ground state. This type of symmetry breaking is specific to finite nuclei and does not arise in nuclear matter.

Breaking of Charge Symmetry in a Finite Nucleus

As was noted in Ref. 30, one of the problems in nuclear structure is the problem of the Coulomb energy. Nolen and Schiffer[31] noted that there is an approximately 8% discrepancy in calculations of the mass difference for mirror nuclei or the mass difference between a nucleus and its analog. The reason for this anomaly has been intensively discussed since then. Numerous mechanisms have been proposed for its explanation: a lower valency of the orbits, core polarization, an interaction that violates the charge symmetry, and so forth. Measurement of the difference between the radii in the proton and neutron distributions in nuclei could help to solve this problem. Numerous studies have been devoted to the extraction of this difference from data on high-energy scattering of protons, pions, and other particles. However, the uncertainties in the interpretation of the data make it as yet impossible to draw clear conclusions. It remains unclear whether the Hartree–Fock method yields a correct calculation for the difference between the neutron and proton radii.

In 1974, Nir[32] showed that there is a correlation between the Coulomb energy shift and the binding energy through the complete periodic system. Both these quantities, which characterize general properties of nuclei, depend on the position of the nucleus in the periodic table and on the quantum numbers of the nuclear state. They also depend similarly on shell effects. Hartree–Fock calculations do not take into account many-particle effects of such type.

The effective interaction determined by the matrix elements (95) is directly related to the binding energy through the channels c that describe the real and virtual decays of the considered nuclear state. It depends on the charge even in the cases when H_{QQ} is charge-symmetric, since the decay thresholds for the protons and neutrons are different. The magnitude of the violation of charge symmetry in H_{QQ}^{eff} is directly related to the difference between the neutron and proton binding energies. Therefore, the effective interaction determined by (95) depends strongly on the nuclear structure, i.e., it contains shell effects.

The numerical calculations of Ref. 33 made in the shell model in the continuum showed that the number of channels taken into account has a strong influence on the Coulomb shift. This is illustrated by the results for the case $^{15}\mathrm{N}$–$^{15}\mathrm{O}$ given in Table II. The calculations were made with the residual interaction (52) with the parameters $V_0 = -650$ MeV/F^3 and $a_b = 0.30$, $b_b = 0.24$ for the bound states and

TABLE II. Dependence of the energy shift Δ on the number of channels taken into account in the calculation.

Number of channels				Δ, MeV
^{15}N		^{15}O		
^{14}C + p	^{14}N + n	^{14}N + p	^{14}O + n	
4	7	7	1	0.42
3	7	7	1	0.22
2	7	7	1	−0.07

$a_s = 0.70$, $b_s = 0.30$ for the decay states. Thus a certain dependence on the density was introduced into the residual interaction. It was assumed that the ^{15}N and ^{15}O ground states are $1p_{1/2}$ hole states. The normal-parity states of the ^{14}N, ^{14}C, and ^{14}O nuclei were constructed from the shell-model states $1p_{3/2}$ and $1p_{1/2}^2$, as in Refs. 34 and 35. States with different parity were not taken into account. The unbound single-particle states were calculated in the same Woods–Saxon potential as the bound states. The single-particle $d_{3/2}$ resonance was truncated at 7.5 F. The number of channels taken into account was restricted to the lowest states of the final $A = 14$ nuclei (Fig. 4). The energy shift between the analog states resulting from the coupling of the discrete states to the continuum is

$$\Delta = F_R(^{15}\mathrm{O}) - \Delta F_R(^{15}(\mathrm{N}). \quad (96)$$

This quantity characterizes the charge dependence of the effective Hamiltonian described by (95). It gives an additional contribution to the Coulomb energy shift of the two mirror nuclei. The magnitude depends strongly on the number of channels taken into account in the calculation (see, for example, Table II in Ref. 33).

There are two possibilities for truncating the continuum in numerical calculations:.

a) an equal number of channels in ^{15}N and ^{15}O is taken, i.e., the analog states are taken into account in the same manner;

b) the continuum is truncated at the same energy, i.e., all channels below a certain energy are taken into account.

The numerical results of Ref. 33 show that a suitable truncation of the continuum lies between these two extreme cases. The difference between them is due to the difference between the Coulomb energies of the two nuclei ^{14}C and ^{14}O. The ^{14}N nucleus is manifested both in $\Delta E_R(^{15}\mathrm{O})$ and in $\Delta E_R(^{15}\mathrm{N})$, and therefore there is virtually no contribution from it to (96).

It is immediately seen that the effects of a closed shell must be manifested in the Coulomb energy shifts: For nuclei with one nucleon outside closed shells the neutron or proton separation coefficients are dominant, and the binding energy of these channels is small. Therefore, analog channels associated with one and the same final nucleus having a closed shell determine the shifts for both nuclei, so that their difference Δ (96) and the charge dependence of the effective nuclear force are small. In contrast, in nuclei with one hole in closed shells both a proton and a neutron channel associated with different final nuclei are important. Therefore, for such nuclei the charge dependence of the effective nuclear force is strongly manifested. Thus, the Coulomb energy shift, like the binding energy, decreases strongly at the beginning of each shell. This corresponds to the effects noted in Ref. 32 in the analysis of experimental data.

Figure 5 shows the difference between the binding energies for $A \to (A-1) + n$ and $A \to (A-1) + p$ for nuclei with $7 \leqslant A \leqslant 41$. We observe a regularity in its behavior with $\Delta A = 4$. Consider the ground states of even-A nuclei. For the nuclei consisting of $4n + 1$ nucleons (n integral), the difference $Q^{(n)} - Q^{(p)}$ is significantly larger for nuclei with $T_z = (1/2)(N - Z) = -1/2$, than for nuclei with $T_z = 1/2$.

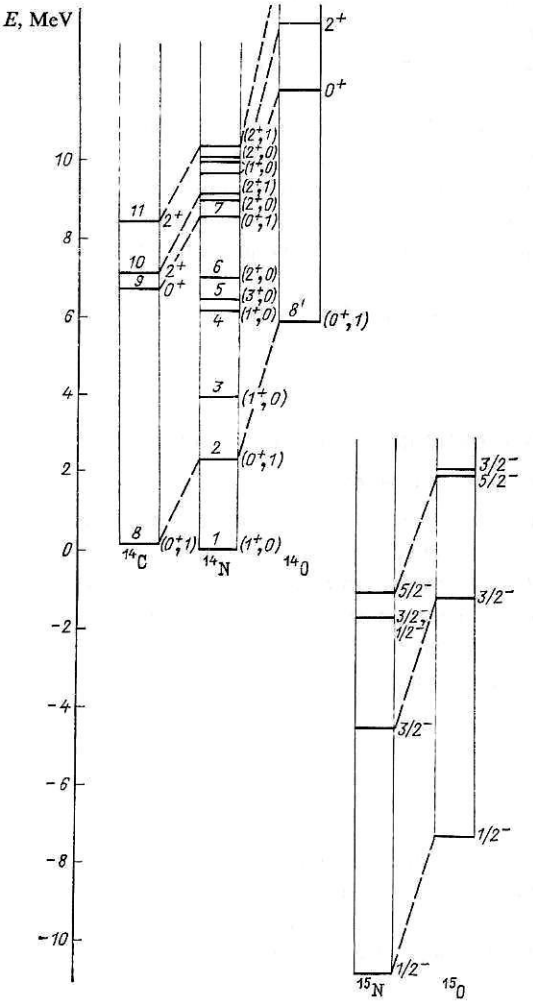

FIG. 4. Level schemes of the nuclei ^{14}C, ^{14}N, and ^{14}O and the level positions relative to the ground states of the nuclei ^{15}N and ^{15}O.

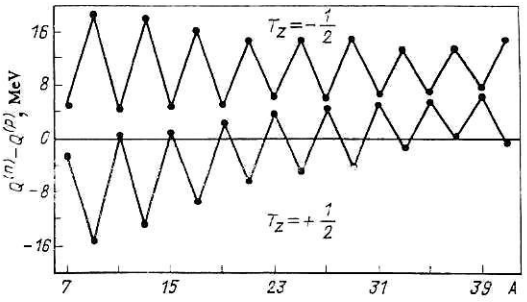

FIG. 5. Differences between the binding energies of neutrons, $Q^{(n)}$, and protons, $Q^{(p)}$, for light nuclei $[T_z = \frac{1}{2}(N - Z)]$. The data are taken from Ref. 58.

Therefore, the charge dependence of the effective nuclear force is greater for nuclei with $T_z = 1/2$ than for nuclei with $T_z = 1/2$. For nuclei with $4n - 1$ nucleons, the value of $Q^{(n)} - Q^{(p)}$ for nuclei with $T_z = -1/2$ and $T_z = -1/2$ is much smaller. Therefore, the charge dependence of the effective nuclear force is relatively large in these nuclei.

Thus, the Coulomb energy shifts for nuclei with $4n + 1$ nucleons and $4n - 1$ nucleons differ systematically.[36] This effect is well known from the analysis of the experimental data as the even–odd effect[31,37] and is interpreted as a consequence of Coulomb pairing effects, i.e., it is assumed that there is an additional Coulomb energy shift for paired protons.[37] It should however, be noted that the observed differences in the Coulomb energy shifts between neighboring nuclei behave like the binding energies. This correspondence indicates the existence of charge-dependent effective nuclear forces, which were discussed above without the introduction of additional phenomenological forces.

In Sec. 2, the width of the isospin/forbidden decay of the $3/2^-$, 3/2 level for ^{13}N was investigated. It was shown[19] that the coupling of two channels strongly influences the width (see Table I) because of the presence of the charge-symmetry breaking part ω_R in the wave function of the decay state in accordance with (67), (82), and (83), or, in other words, because of the charge-asymmetric part $H^{\text{eff}}_{QQ} - H_{QQ}$ of the Hamiltonian (95). It can therefore be expected that in the case of isospin-forbidden transitions there will be A dependences similar to those for the Coulomb energy shift.

The experimentally observed behavior in the isospin-forbidden decays indicates that the isospin mixing is not primarily due to fortuitous degeneracy of states with different isospin but is the result of a mechanism that reflects general properties of nuclear structure.[38] Investigation of the widths of isospin-nonconserving decays in light nuclei brings to light the following behavior. For nuclei with $A = 4n + 1$ nucleons the reduced widths of the neutron decays of the lowest levels with isospin $T = 3/2$ and $T_z = 1/2$ are usually approximately ten times greater than the widths of the analog proton decays of the nuclei with $T_z = -1/2$. In Ref. 39, this effect was explained in terms of matrix elements between analog states and their antianalog configurations. However, it follows from Fig. 5 that for nuclei with $A = 4n + 1$ the charge dependence of the nuclear forces in the case $T_z = -1/2$ is significantly less than for the analog nuclei with $T_z = 1/2$. Therefore, the neutron decay widths must be greater than the analog proton decay widths.

Discussion of the $\Delta A = 4$ features can of course explain only general features of the charge-dependent effects. For each specific nucleus there will be certain deviations due to the spectroscopic factors and the density of the levels in the final nuclei at low excitation energies. Certain regularities in such deviations are observed both in the experimentally measured Coulomb energy shifts[37] and in the widths of the isospin-nonconserving decays.[40] For their explanation, it is necessary to make calculations in the shell model in the continuum. More detailed experimental data are necessary. The observed $\Delta A = 4$ features in the widths of isospin-nonconserving decays and also in the Coulomb energy shift can be explained by variations in the number of channel wave functions taken into account.

Because of the difference between the neutron and proton wave functions, the wave functions $\Omega_R = \Phi_R + \omega_R$ of the resonance states of mirror nuclei are not coupled by an isospin raising or lowering operator. The additional difference in the wave functions Ω_R is only to a small degree due to the difference between the parameters of the Woods–Saxon potential for protons and neutrons. This can be seen from the results of the calculations of Ref. 19 for nuclei with $A = 12$ and 13 given in Sec. 2, in which the parameters were taken to be the same. Basically, the difference is due to the Coulomb single-particle interaction. Moreover, the difference between the neutron and proton wave functions leads to an energy shift in the mirror nuclei. Such a shift was described in Ref. 41 by the introduction of a phenomenological charge-symmetry violating nuclear interaction. In the shell model in the continuum there is no need for the phenomenological introduction of such an interaction. It arises naturally from the coupling between the discrete and continuum states.

Thus, correct allowance for the coupling between the discrete states and the continuum states leads to a charge dependence of the nuclear forces in the subspace of the discrete states. The general properties of the charge dependence can be determined by considering the analytic expression for the effective Hamiltonian. The charge-dependence effect is directly related to the appropriate allowance for the number of channel wave functions describing the neutron decay and proton decay (virtual or real) of the nuclear states. As a function of A, the charge dependence behaves like the binding energy, i.e., in the shell model in the continuum the appearance of shell effects in the charge dependence is explained naturally. This part of the charge dependence of the nuclear forces is a consequence of the finiteness of the nuclear system.

Symmetry Violation of Nucleon and Δ-Isobar Correlations in Finite Nuclei

One of the tasks of nuclear physics is to study spin-isospin correlations in nuclei; these play an important part in the excitation of pionlike states. Such states are a strong mixture of nucleon–hole and isobar–hole (NN^{-1} and ΔN^{-1}) excitations. In the majority of calculations, the average interaction forces for the $NN^{-1} \leftrightarrow NN^{-1}$, $NN^{-1} \leftrightarrow \Delta N^{-1}$, and

TABLE III. Positions E_R^{SM}, shifts ΔE_R, and widths Γ_R of the J^π, $T=1^-$, 1 states in the ^{16}O nucleus, calculated with four channels.

$E_R^{(exp)}$, MeV	E_R^{SM}, MeV	ΔE_R, MeV	Γ_R, MeV
17.5	17.72	−0.25	0.27
19.0	20.43	−0.50	0.05
22.5	24.14	−1.77	1.52
25.0	25.70	−0.84	1.48

$\Delta N^{-1} \leftrightarrow \Delta N^{-1}$ correlations are taken to be the same by virtue of the universality of the spin–isospin correlations that follows from the naive quark model and from SU(2)×SU(2) symmetry.[42] Microscopic calculations made for infinite nuclei[43] appear to confirm this assumption. Indirectly, this is confirmed by the part played by the Δ isobar in suppressing spin–isospin transitions if the entire suppression is due to the ΔN^{-1} screening mechanism,[42,44] or, which is equivalent, a shift of an appreciable fraction of the strength of the Gamow–Teller forces to energies significantly beyond the Gamow–Teller resonance.

Despite the fact that the above assertions concerning the relative importance of the $NN^{-1} \leftrightarrow NN^{-1}$, $NN^{-1} \leftrightarrow \Delta N^{-1}$ and $\Delta N^{-1} \leftrightarrow \Delta N^{-1}$ correlations are in apparent agreement, some questions remain open. Suppression effects of the same order of magnitude as in the transition to pionlike states are well known in transitions in which there are no contributions from a Δ–h component. For example, there has been a long discussion of the problem of the disappearance of the strength in photonuclear reactions on light nuclei. Such an effect is also known in the case of inelastic scattering of pions, protons, and electrons. The suppression effect in Fermi transitions was discussed in very precise measurements of isobar analog resonances.[46] Its magnitude is of the same order as in the Gamow–Teller transitions, despite the fact that the analog resonances are not pionlike states. It is important that the restrictions which follow from the unitarity of the S matrix on the reaction cross sections are usually not fully taken into account in the analysis of the data. For this reason, as was shown in Ref. 47, a suppression effect arises erroneously in the data. Such a source of "suppression" for a wide range of nuclei is characterized by a smooth dependence on the mass number and on the angular momentum like the suppression effect induced by the Δ-isobar degree of freedom. Therefore, it may be assumed that only part of the suppression in the isovector spin transitions is due to the Δ–h screening mechanism.

Microscopic calculations were made for finite nuclei for which the greater part of the excited states have a short lifetime compared with the decay to nucleon channels. In this case, there is a certain breaking of the symmetry in the NN and ΔN interactions absent in nuclear matter. This difference between the NN and ΔN correlations which arises here because of the coupling between the discrete states and the continuum states, corresponds to the difference between the effective nuclear forces used, for example, in the shell model and in the shell model in the continuum.

The influence of the finite lifetime of the excited nuclear states on the results of traditional calculations of nuclear structure was investigated numerically for the $^{16}O(\gamma, N)$ reaction with 1^- states having $1p1h$ structure.[48] It follows from the results that the effective nuclear forces employed in these calculations must be significantly changed in order to obtain the same excitation spectrum in both the standard shell model and the shell model in the continuum. The numerical values of the energy shifts ΔE_R due to $H_{QQ}^{eff} - H_{QQ}$ in the $A = 16$ nuclei for a number of levels with $1p1h$ structure are given in Table III, and for levels with $2p2h$ structure in Table IV (configuration space: $1s_{1/2}$, $1p_{3/2}$, $1p_{1/2}$, $1d_{5/2}$, $2s_{1/2}$, $1d_{3/2}$). In order of magnitude, the shifts agree with the corresponding values for the widths Γ_R. Although in the general case the energies are not very sensitive to the details of the Hamiltonian, the shifts discussed here are not small.

To describe the particle–hole spin–isospin interaction one usually introduces a parameter g',[49] which takes into account effectively all the correlations except those, such as one- and two-pion exchanges, taken into account explicitly. This parameter is obtained by fitting the experimental data. Therefore, it takes into account all the effects in finite nuclei associated with the finite lifetime of the excited nuclear

TABLE IV. Positions E_R^{SM} and shifts ΔE_R of the J^π, $T=0^+$, 1 states in the ^{16}N nucleus as functions of the number N of channels (Γ_R are the widths calculated for seven channels).

E_R^{SM}, MeV	ΔE_R, MeV				Γ_R, MeV
	$N=1$	$N=2$	$N=4$	$N=7$	
13.73	0	0	−0.02	−0.14	0.20
14.63	0	−0.03	−0.13	−0.13	0.35
15.10	−0.01	−0.01	−0.05	−0.10	0.09
15.48	−0.01	0	−0.01	−0.06	0.09
16.25	0	0.09	−0.10	−0.22	0.28

states. In the majority of calculations,[42,43,50] the parameter is taken to be the same for Δ isobars and for nucleons, although, as was noted above, it should be different for the isobars and nucleons in order to reflect the difference between their coupling to the continuum. An analytic expression for this difference is given by the expression (95).

For stable infinite nuclei the term $H_{QQ}^{\text{eff}} - H_{QQ}$ disappears together with the effects discussed in this subsection. In finite nuclei it leads to a certain symmetry breaking of the system's Hamiltonian.

Surface Effects and Nuclear Radii

One of the main characteristics of nuclei is the distribution of the nucleons in them. Quite a lot is known about the charge distribution, particularly from electron-scattering experiments, but little is known about the neutron distribution. It was assumed that pions would be an effective tool for analyzing the distribution of both the neutrons and the protons. In contrast to the nucleon–nucleon interaction, a single P_{33} wave (Δ_{33} resonance) is dominant in the pion–nucleon interaction in the range of energies from 100 to 300 MeV. It is also important that π^- mesons interact with neutrons more strongly than with protons, while for π^+ it is the other way round. Thus, the π^- are more sensitive to the neutron distribution, and the π^+ to the proton distribution. Therefore, it was expected that comparison of the data for π^+ and π^- would make it possible to obtain direct information about the neutron and proton distributions.

From this point of view, it is of considerable interest to study $\pi^\pm$ scattering by the calcium isotopes ^{40}Ca and ^{48}Ca. A strong effect was expected from the eight neutrons in ^{48}Ca, which are situated outside the ^{40}Ca core. However, it was found[52] that in inelastic scattering low-lying states were excited approximately equally by π^- and π^+ mesons. A similar result was obtained[52] in the case of ^{51}V, which has three protons above a ^{48}Ca core.

In this connection, data on high-energy proton–nucleus scattering were analyzed in Ref. 53. It was shown that the differences between the proton and neutron distributions extracted from these data are in apparent agreement with the estimates that follow from calculations using mean-field theory. The insensitivity of the proton and neutron distributions to the charge of the pions can be attributed to the strong inelasticity (the nucleus is almost black) of the pion–nucleus interaction in the resonance region.

The analysis of the proton-nucleus total reaction cross sections in the region from 100 MeV to 1 GeV made in Ref. 54 showed that they are sensitive to the nuclear density in the region of the effective radius, which is usually larger than the radius at which the density has decreased by a half. Thus, the total reaction cross sections are determined by the edge of the nuclear density. This is a consequence of the fact that the nucleon mean free path in the nucleus is short in this region of energies. Therefore, it is difficult to extract information about the rms nuclear radius from reactions in which the nuclear surface plays the main part.

In this connection, it is of interest to discuss the problem that occurs in the study of α-clustering effects in light and medium nuclei in $(p, p\alpha)$ and $(\alpha, 2\alpha)$ reactions. [5] The problem is that the absolute spectroscopic factors extracted from the $(p, p\alpha)$ reactions agree with the predictions of the shell model, whereas the values obtained from the $(\alpha, 2\alpha)$ reaction are 100 times larger. This discrepancy is attributed to the appearance of α clustering, which develops mainly in the nuclear surface. In the $(\alpha, 2\alpha)$ reaction, the nuclear surface plays the main part, whereas in the $(p, p\alpha)$ processes a greater fraction of the nucleons of the nucleus participate.

One of the advantages of the shell model in the continuum over the traditional shell model is the possibility of taking into account directly surface effects. These effects are described by the additional term ω_R in the wave function of the nuclear state [see Eqs. (67) and (31)]. This term explicitly contains the scattering wave function and the matrix elements $\langle \xi_E^c | H | \Phi_R \rangle$ of the coupling (see Sec. 2). Therefore, the nuclear surface contains virtual particles associated with closed channels. The internal part of the nucleus is described by the wave function Φ_R (see Sec. 2).

According to the shell model in the continuum, transitions from the ground state of nucleus A to an unbound $B + b$ state under the influence of an external field can be described by the matrix elements (37)–(39). The two terms of (38) and (39) contain spectroscopic information about the excited discrete states R that decay into the unbound $B + b$ state. The term (39) describes the change in the wave function of the discrete state R by the continuum. Usually, it is not taken into account in spectroscopic analysis of data, it being assumed that Φ_R is a discrete-state wave function. The term (39) corresponds to the nuclear surface.

The contribution of the channel-resonance scattering term (39) to the cross section and the spectral function was investigated numerically in two cases.

1. The cross section of $^{16}\text{O}(\gamma, n_0)$ photoabsorption with excitation of a giant dipole resonance.[56] The calculations showed that the direct part of the reaction depends smoothly on the energy, and the sum of the direct and the channel–resonance scattering terms has a certain resonance structure (Fig. 6). The total cross section is determined by the resonance part of the reaction. Therefore, for a giant dipole reso-

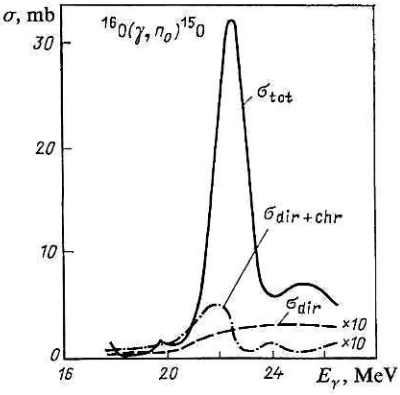

FIG. 6. Giant dipole resonance in the photoneutron reaction on ^{16}O: σ_{tot} is the total cross section, σ_{dir} is the direct part of the cross section, and $\sigma_{\text{dir+chr}}$ is the sum of the direct and the channel–resonance scattering terms in the cross section.

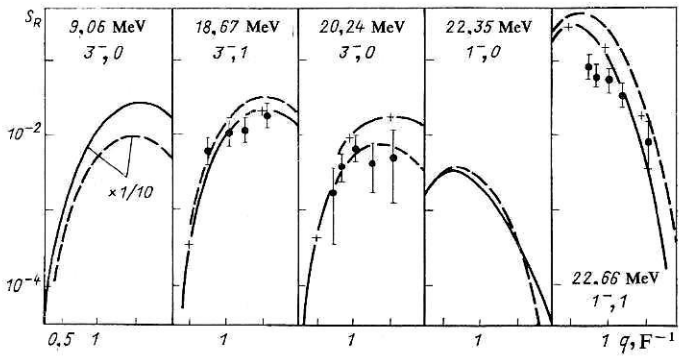

FIG. 7. Spectral function S_R (continuous curves) and its resonance part $S_R^{(\mathrm{res})}$ (broken curves) as functions of the momentum transfer for inelastic electron scattering by ^{12}C with excitation of some resonance states (from Ref. 57).

nance the usually employed approximation of the standard shell model, $\sigma_{\mathrm{tot}} \approx \sigma_{\mathrm{res}}$, is justified.

2. The spectral function for inelastic electron scattering by ^{12}C.[57] In these calculations, the relative contribution of the channel–resonance scattering to the spectral function increases with increasing transfer q (Fig. 7). For $q \geqslant 1$ F^{-1}, the contribution of the channel–resonance scattering term to the spectral function cannot be ignored.

The numerical calculations show that in the general case both terms in the spectral function must be taken into account in calculations at medium energies. Besides the contribution from the open channels, the term (39) takes into account the contributions from the closed channels, the number of which is large. In practical calculations, the number of channels must be limited. The most important channels must be selected not only using energy considerations (the positions of the thresholds ε_c of the channel, c) but also by analysis of the structure (the spectroscopic factor of the state Φ_R with respect to ξ^c). Calculations of nucleon–nucleus reactions at low energies show that the two criteria are equally important. Since little is known about the properties of the closed channels, experimental indications are necessary for their selection in numerical calculations.

We list the general properties of the channel–resonance scattering term (39) or (43) in the spectral function.

1. It takes into account the coupling of the channels not only to the open but also to the closed channels. This type of channel coupling differs from the channel coupling which arises from the inclusion of higher states of the shell model, which are in reality unbound, as well as from the approach in which the channel coupling arises through the inelastic coupling of the incident particle and excited states. The channel coupling considered here determines the properties of the investigated state, since it is contained in Ω_R. Therefore, it is characteristic of the state.

2. In accordance with (40), this type of coupling reflects averaged characteristics of the system, since it contains a sum over all channels and an integral over the energies. Therefore, the sum $A_R^{(\mathrm{res})} + A_R^{(\mathrm{chr})}$ in the spectral function S_R (41) is more or less constant for nuclei with similar structure and energies ε_c of the cluster thresholds. Neglect of the term $A_R^{(\mathrm{chr})}$ in data analysis leads, therefore, to distortion of the absolute values of the spectroscopic factors of these nuclei, but does not change their relative magnitudes too strongly.

3. The channel–resonance scattering term is important at the periphery of the nucleus. Data analysis without allowance for it should be done using radii larger than the rms radius. The real radius depends on the relationship between $A_E^{(\mathrm{res})}$ and $A_R^{(\mathrm{chr})}$.

4. Its contribution to the spectral function depends on the energies ε_c of the thresholds and on the separation coefficients for decays to the channels c′ for which the matrix elements $\langle \xi_E^{c'} | F \rangle$ are large. Therefore, neglect of the channel–resonance scattering term in the analysis of different reactions may lead to differences in the absolute magnitudes of the spectroscopic factors.

It follows from the listed properties that the enhancement of virtual α clustering in the nuclear surface observed in α-nuclear reactions may be due to the ω_R term in the wave function of the nuclear states. This interpretation is supported by the fact that analysis with a radius greater than the rms radius does not lead to enhancement. Moreover, the relative spectroscopic factors for transitions to the ground states of nuclei with low-lying thresholds for α decay agree with one another, as must be the case in accordance with (41). Because of the strongly surface nature of α -nuclear reactions, α clustering in the surface of nuclei with low-lying α-decay thresholds is more pronounced than in nucleon-nuclear reactions.

For nuclei with low-lying α-decay channels, there is a difference between the average values of the spectroscopic factors obtained, respectively, in proton-nuclear and α-nuclear knockout reactions. In ^{16}O, for example, the threshold for the $^{12}C_{gs} + \alpha$ decay channel is at 7.2 MeV and for $^{12}C_{4.4\mathrm{MeV}} + \alpha$ it is at 11.6 MeV, whereas the nucleon channel opens at higher energies. Moreover, the corresponding spectroscopic factors $^{16}O_{gs}$ are larger than the nucleon spectroscopic factors. Therefore, in ω_R the α channels are important, and this leads to the enhancement of the α clustering in the ^{16}O surface, for which the channel–resonance scattering term (39) is responsible.

To prove the above assertions, it would be very interesting to have experimental data not only for nuclei with low-lying cluster thresholds but also for nuclei having low-lying nucleon thresholds. For example, for ^{13}N the $^{12}C + p$ decay channel has threshold 1.9 MeV, while the $^{9}B + \alpha$ channel has threshold 9.5 MeV. In this case, the surface of the nucleus is enriched with nucleons and not clusters. One must therefore expect here a value smaller than in the case of ^{16}O for the ratio of the α-spectroscopic factors extracted from reactions with the participation of α particles and protons

when the rms radius is used.

For more definite conclusions about the part played by the term ω_R, we need more experimental data for different nuclei. Study of the ω_R term by means of the knockout reaction will make it possible not only to draw conclusions about the enhancement of the clustering in the nuclear surface but also to settle such difficult questions as the problem of the absolute magnitude of the α width in heavy nuclei (see Sec. 2) and the problem of determining the proton and neutron distributions in nuclei from π-nuclear data.

The symmetry relations established in reactions with particles of intermediate energies characterize not only the interior region of the nucleus but also its surface. The ratio of the two terms (38) and (39) depends on the mean free path of the incident particle, i.e., on its species and energy. Analyzing data obtained from different reactions at intermediate energies, it is possible to study the properties of the interior region of the nucleus and its surface.

The symmetry properties of the surface are determined by the threshold energies of the channels and their fractional -parentage relation to the considered state. They differ from the symmetry properties of the interior part of the nucleus, which is determined by the total numbers of protons and neutrons. An example is provided by the ^{40}Ca and ^{48}Ca nuclei, whose surfaces, as nuclei with closed shells, are similar, while the interior parts differ because of the different numbers of protons and neutrons.

The surface properties characterize finite nuclei. They are determined by general properties of the many-particle system such as the binding energy and coefficients of separation in the corresponding decay channels, and they can be considered analytically in the framework of a model that describes bound and unbound states in a unified way.

4. CONCLUSIONS

Nuclear-structure calculations are usually made by diagonalizing the Hamiltonian in the space of bound single-particle states. Because of this, one loses sight of the characteristic properties of a nucleus that distinguish it from infinite nuclear matter. Characteristics such as the lifetimes of excited states and surface effects are calculated by means of approximations whose validity is limited.

In the present paper, besides bound states, we have considered low-lying decay channels, which characterize the finiteness of the nuclear system. We have obtained an analytic expression describing the surface of the nucleus. It arose in the form of an additional term in the wave function of the nuclear state, and it contains information about both the open and closed decay channels. Such a change in the nuclear wave functions by the continuum is analogous to the change in scattering states brought about by taking into account the discrete spectrum of the system in the unified theory of nuclear reactions formulated by Feshbach.[4]

The Hamiltonian describing the nuclear structure of the decay states is non-Hermitian. The non-Hermitian part of the Hamiltonian has an essentially many-particle nature and cannot be taken into account by changing the residual two-particle interaction. The eigenvalues of this Hamiltonian determine both the energies and the lifetimes of the nuclear states. The effective Hamiltonian obtained here leads to some symmetry breakings such as breaking of the charge symmetry and the symmetry of the NN^{-1} and ΔN^{-1} interactions. Analysis shows that the parameters g′ describing the spin–isospin NN^{-1} and ΔN^{-1} interactions in finite nuclei must be different, in contrast to nuclear matter. However, it is true that this difference may be less than Migdal's prediction.[49]

Another consequence of the unified description of bound and unbound states is the deviation of the line shape of the resonance states from the Breit–Wigner and Lorentz shapes even in the absence of interference effects with other resonance states and with the background. As a limiting case, the resonances may appear in the cross section in the form of cusps.

All the results discussed in the present paper were obtained numerically in the framework of the shell model in the continuum using realistic wave functions for light nuclei. The scheme is a natural generalization of the standard shell model. The approximations used in the calculations were truncation of the function space, the use of a simplified two-particle residual interaction, and the limitation to single-nucleon decay channels. The results obtained were compared qualitatively with the experimental data. The comparison indicated the possibility of explaining effects such as the closed-shell effects in the breaking of the charge symmetry of the nuclear forces, and also some surface effects. For quantitative predictions, it is necessary to include in the calculations the low-lying α-decay channels and to use a more realistic two-particle interaction. A scheme for including α channels was discussed in Ref. 16, though it does require more computing time. A more realistic two-particle residual interaction must depend on the density in the description of the nucleon–nucleon interaction both without and within the nucleus. Numerical calculations for specific nuclei can be made only when more experimental data are available to indicate where one must make a sensible truncation in the number of closed channels.

The surface effects discussed in the present paper may play an important role in heavy-ion reactions, in which the surface properties of the nuclei are particularly important. They are also important, for example, in the pion-nucleus interaction when the interaction takes place mainly on the surface of the nucleus. Knockout reactions are of particular interest from the point of view of obtaining information about the nuclear surface and effects associated with it.

For fruitful discussions I am indebted to V. V. Balashov, H. W. Barz, and R. Wünsch.

[1]H. W. Barz, I. Rotter, and J. Höhn, Nucl. Phys. **A275**, 111 (1977).
[2]C. Mahaux and H. A. Weidenmüller, Shell-Model Approach to Nuclear Reactions, North-Holland, Amsterdam (1969).
[3]W. L. Wang and C. M. Shakin, Phys. Lett. **32B**, 421 (1970).
[4]H. Feshbach, Ann. Phys. (N.Y.) **19**, 287 (1962).
[5]R. H. Lemmer and C. M. Shakin, Ann. Phys. (N.Y.) **27**, 13 (1964).
[6]J. Hüfner and R. H. Lemmer, Phys. Rev. **175**, 1394 (1968).
[7]C. Mahaux and A. M. Saruis, Nucl. Phys. **A177**, 103 (1971).
[8]D. Robson and A. M. Lane, Phys. Rev. **161**, 982 (1967).
[9]D. Robson, Phys. Rev. **137**, 1535 (1965).

[10]A. Mekjian and W. MacDonald, Nucl. Phys. **A121**, 385 (1968).
[11]H. L. Harney, H. A. Weidenmüller, and A. Richter, Phys. Rev. C **16**, 1774 (1977).
[12]P. E. Vorotnikov, Yu. V. Melikov, Yu. D. Otstavnov, *et al.*, Yad. Fiz. **17**, 901 (1973) [Sov. J. Nucl. Phys. **17**, 471 (1973)].
[13]J. U. Andersen, K. O. Nielsen, J. Skak-Nielsen, *et al.*, Nucl. Phys. **A241**, 317 (1975).
[14]B. N. Bugrov, V. V. Kamanin, S. A. Karamyan, *et al.*, Yad. Fiz. **25**, 713 (1977) [Sov. J. Nucl. Phys. **25**, 379 (1977)].
[15]E. P. Kanter, D. Kollewe, K. Komaki, *et al.*, Nucl. Phys. **A299**, 230 (1978).
[16]I. Rotter, Phys. Rev. C **27**, 2261 (1983).
[17]A. Arima and S. Yoshida, Nucl. Phys. **A161**, 492 (1971).
[18]R. E. Marrs, E. G. Adelberger, and K. A. Snover, Phys. Rev. C **16**, 61 (1977).
[19]I. Rotter, J. Phys. G **5**, 75 (1979).
[20]G. J. Wagner, K. T. Knöpfle, G. Mairle, *et al.*, Phys. Rev. C **16**, 1271 (1977).
[21]I. Rotter, Ann. Phys. (Leipzig) **38**, 221 (1981).
[22]J. P. Jeukenne and C. Mahaux, Nucl. Phys. **A136**, 49 (1969).
[23]I. Rotter, J. Phys. G **5**, 685 (1979).
[24]I. Rotter, Lect. Notes Phys. **156**, 233 (1982).
[25]I. Rotter, H. W. Barz, and J. Höhn, Nucl. Phys. **A297**, 237 (1978).
[26]H. W. Barz and I. Rotter, Nukleonika **20**, 413 (1975); I. Rotter, H. W. Barz, R. Wünsch, and J. Höhn, Fiz. Elem. Chastits At. Yadra **6**, 435 (1975) [Sov. J. Part. Nucl. **6**, 175 (1975)].
[27]P. R. Malmberg, Phys. Rev. **101**, 114 (1956); L. Brown, E. Steiner, L. G. Arnold, and R. G. Seyler, Nucl. Phys. **A206**, 353 (1973).
[28]K. M. McVoy, Nucl. Phys. **A115**, 481, 495 (1968); C. J. Goebel and K. W. McVoy, Nucl. Phys. **A115**, 504 (1968).
[29]I. Lovas and E. Dénes, Phys. Rev. C **7**, 937 (1973).
[30]G. Bertsch, L. Zamick, and A. Mekjian, Lect. Notes Phys. **119**, 240 (1979).
[31]J. A. Nolen and J. P. Schiffer, Ann. Rev. Nucl. Sci. **19**, 471 (1969).
[32]D. Nir, Can. J. Phys. **52**, 2132 (1974).
[33]B. Kämpfer and I. Rotter, J. Phys. G **5**, 747 (1979).
[34]D. Kurath, Phys. Rev. **106**, 975 (1957).
[35]A. N. Boyarkina, Izv. Akad. Nauk SSSR, Ser. Fiz. **28**, 337 (1964).
[36]I. Rotter, J. Phys. G **6**, 185 (1980).
[37]D. Nir, Nucl. Phys. **A194**, 103 (1972).
[38]P. G. Ikossi, K. A. Snover, J. L. Osborn, and E. G. Adelberger, Nucl. Phys. **A319**, 109 (1979).
[39]A. B. McDonald and E. G. Adelberger, Phys. Rev. Lett. **40**, 1692 (1978).
[40]P. G. Icossi, W. J. Thompson, T. B. Clegg, *et al.*, Phys. Rev. Lett. **36**, 1357 (1976).
[41]H. Sato, Nucl. Phys. **A269**, 378 (1976); **A304**, 477 (1978).
[42]W. Weise, Nucl. Phys. **A374**, 505 (1982) (Proc. of the 9th ICOHEPANS, Versailles, France, 1981).
[43]H. Müther, in: Proc. of the 19th Intern. Winter Meeting on Nuclear Physics, Bormio, Italy (1981), p. 638.
[44]E. Oset and M. Rho, Phys. Rev. Lett. **42**, 47 (1979); I. S. Towner and F. C. Khanna, Phys. Rev. Lett. **42**, 51 (1979).
[45]A. Bohr and B. Mottelson, Phys. Lett. **100B**, 10 (1981).
[46]E. G. Bilpuch, A. M. Lane, G. E. Mitchell, and J. D. Moses, Phys. Rep. **28C**, 145 (1976).
[47]P. Kleinwächter and I. Rotter, Nucl. Phys. **A391**, 137 (1982).
[48]H. W. Barz, J. Birke, and H. J. Eger, Yad. Fiz. **24**, 508 (1976) [Sov. J. Nucl. Phys. **24**, 264 (1976)].
[49]A. B. Migdal, Rev. Mod. Phys. **50**, 107 (1978).
[50]J. Meyer-ter-Vehn, Phys. Rep. **74**, 323 (1981); W. H. Dickhoff, A. Faessler, J. Meyer-ter-Vehn, and H. Müther, Phys. Rev. C **23**, 1154 (1981); J. Delorme, Nucl. Phys. **A374**, 541 (1982) (Proc. of the 9th ICOHEPANS, Versailles, France, 1981).
[51]M. B. Johnson and H. A. Bethe, Comments Nucl. Part. Phys. **8**, 75 (1978).
[52]R. A. Eisenstein, in: High-Energy Physics and Nuclear Structure, Seventh Intern. Conf. (ed. M. P. Locher) Zürich (1977), p. 209.
[53]J. W. Negele, L. Zamick, and G. K. Varma, Comments Nucl. Part. Phys. **8**, 135 (1979).
[54]D. J. Ernst, Phys. Rev. C **19**, 896 (1979).
[55]C. Samanta, N. S. Chant, P. G. Roos, *et al.*, Phys. Rev. C **26**, 1379 (1982).
[56]J. Höhn, H. W. Barz, and I. Rotter, Zfk-350 (Rossendorf, 1978), p. 67.
[57]R. Wünsch, V. L. Korotkikh, and N. N. Titarenko, Yad. Fiz. **29**, 318 (1979) [Sov. J. Nucl. Phys. **29**, 157 (1979)].
[58]F. Ajzenberg-Selove and T. Lauritsen, Nucl. Phys. **A227**, 1 (1974); F. Ajzenberg-Selove, Nucl. Phys. **A248**, 1 (1975); **A268**, 1 (1976); **A281**, 1 (1977); **A300**, 1 (1978); P. M. Endt and C. Van der Leun, Nucl. Phys. **A214**, 1 (1973).

Translated by Julian B. Barbour